

IMIDAZOLINE SCAFFOLDS AS SMALL MOLECULE INHIBITORS OF THE HUMAN  
PROTEASOME

By

Lauren Marie Azevedo

A THESIS

Submitted to  
Michigan State University  
in partial fulfillment of the requirements  
for the degree of

Pharmacology and Toxicology – Master of Science

2014

## ABSTRACT

### IMIDAZOLINE SCAFFOLDS AS SMALL MOLECULE INHIBITORS OF THE HUMAN PROTEASOME

By

Lauren Marie Azevedo

In the past decade, modulating NF- $\kappa$ B activation through inhibition of the proteasome has emerged as a therapeutic target for the treatment of malignancies and autoimmune diseases. In 2003, the proteasome inhibitor bortezomib was approved by the FDA for the treatment of the plasma cell neoplasm, multiple myeloma. Although bortezomib effectively treats multiple myeloma and has shown promising results for the treatment of these other diseases, its therapeutic potential is limited by peripheral neuropathy, reduced activity in solid tumors, and route of administration restrictions. In 2004, the Tepe laboratory first identified the imidazoline scaffold, as an inhibitor of the NF- $\kappa$ B pathway and subsequently identified the proteasome as its target. The studies presented in this thesis show that the noncompetitive imidazoline proteasome inhibitor, TCH-013, is bioavailable and not hepatotoxic. This compound was also shown to have anti-inflammatory properties and to reduce the bronchoalveolar lavage fluid cellularity in an experimental model of asthma. In addition, we enhanced the efficacy of this molecule by manipulating the functional groups. The result of these studies is the discovery of compound 43, a noncompetitive proteasome inhibitor that is able to overcome bortezomib resistance, is bioavailable, and is effective in an animal model of systemic inflammation. The data presented herein suggest that a modified imidazoline scaffold is an effective, noncompetitive and nontoxic proteasome inhibitor that has therapeutic potential for the treatment of multiple myeloma and asthma.

Copyright by  
LAUREN MARIE AZEVEDO  
2014

For my father, John Azevedo, who introduced me to the magic of science and the wonders of medicine.

## ACKNOWLEDGEMENTS

I would like to first thank my mentor, Dr. Jetze Tepe. Over the years, he has spent countless hours helping me develop into an independent and focused researcher. I appreciate his understanding and willingness to take a chance on a multi-disciplinary student. Without his support, inside and outside of the lab, this work would not have been possible.

I would also like to thank my committee members, Dr. Norbert Kaminski, Dr. Patricia Ganey, and Dr. Anne Dorrance. They have been a strong support network since my first interview and I sincerely appreciate all of the time and effort they have put into my education and professional development.

I would like to thank the College of Osteopathic Medicine, the DO/PhD program and the Department of Pharmacology and Toxicology at Michigan State for the unfaltering support. Special thanks goes to Dr. Justin McCormick, Ms. Bethany Heinlen, Dr. Keith Lookingland, Dr. Anne Dorrance, and Dr. Celia Guro for taking special interest in my career and personal development. I would also like to thank the support staff for their help with everything over the years.

I would like to acknowledge the collaborators that made these projects possible. First, to Dr. Bill Henry, Dr. Jack Harkema, Dr. Jim Wagner and Dr. John Lapres who spent countless hours laying the groundwork for this research. To the lab members, especially Dr. Steve Proper and Dr. Devan Jackson-Humbles who taught me the techniques and supported me throughout the studies.

I would like to thank my lab members and friends who have given me so much emotional and intellectual support throughout this process. I owe a deep debt of gratitude to the Tepe Lab and its members for their help with chemistry, and to Teri Lansdell who is an amazing person and mentor. I would especially like to thank my closest friends, Nicole Hewlett, Sujana Pradhan, Mike Strug, Emilia Boffi and Britany Brutsche for everything they have done to make this possible.

Finally, I would like to thank my entire family for their unconditional love and support. To my grandmother, you have inspired me to go above and beyond whatever I thought I could achieve and I appreciate everything you have done for our family throughout the years. To my mother and step-father, your love and support throughout my entire life has made me the person that I am today. To my husband and best friend, Ryan Keating, who believes in me no matter what, I would have not made it through this without you.

## TABLE OF CONTENTS

|   |            |
|---|------------|
| <b>LIST OF TABLES .....</b>   | <b>ix</b>  |
| <b>LIST OF FIGURES.....</b>   | <b>x</b>   |
| <b>KEY TO ABBREVIATIONS .....</b>   | <b>xii</b> |
| <b>CHAPTER 1- INTRODUCTION .....</b>  | <b>1</b>   |
| The ubiquitin-proteasome system .....   | 1          |
| Identification of the imidazoline scaffold as an inhibitor of NF- $\kappa$ B through modulation of the proteasome .....   | 3          |
| The role of NF- $\kappa$ B in asthma and the proteasome inhibitor as potential steroid sparing therapy .....  | 4          |
| Disruption of NF- $\kappa$ B signaling through proteasome inhibitors as treatment for multiple myeloma .....  | 5          |
| <b>CHAPTER 2- MATERIALS AND METHODS .....</b>   | <b>9</b>   |
| Reagents .....  | 9          |
| Cell culture .....  | 9          |
| Animals and husbandry .....   | 9          |
| OVA-induced allergic airway model .....   | 10         |
| Pulmonary function analysis .....   | 11         |
| Cytokine bead array .....   | 11         |
| Enzymatic activity assessment .....   | 11         |
| Cytotoxicity measurement .....  | 12         |
| Development of bortezomib resistant cell lines .....  | 12         |
| Bioavailability .....   | 13         |
| ALT assay .....   | 14         |
| LPS challenge .....   | 14         |
| ELISA .....   | 14         |
| Statistical analysis .....  | 15         |
| <b>CHAPTER 3- RESULTS AND DISCUSSION .....</b>  | <b>16</b>  |
| TCH-013 is bioavailable, non-toxic and disrupts the inflammatory cellular profile of BALF but not airway hyperresponsiveness in an experimental model of asthma ..... | 16         |
| Modification of the imidazoline scaffold yielded a molecule with increased efficacy and a noncompetitive binding profile .....  | 38         |
| The modified imidazoline is cytotoxic and overcomes bortezomib resistance in cell culture of multiple myeloma .....   | 45         |
| Compound 43 is bioavailable and attenuates the systemic inflammatory response <i>in vivo</i> .....  | 49         |

|   |           |
|---|-----------|
| <b>CHAPTER 4- SUMMARY AND CONCLUSIONS .....</b> | <b>53</b> |
| <b>Limitations and future directions.....</b>   | <b>53</b> |
| <b>Conclusion.....</b>                          | <b>54</b> |
| <b>BIBLIOGRAPHY .....</b>                       | <b>56</b> |



## LIST OF TABLES

|   |           |
|---|-----------|
| <b>Table 1. The role of cytokines in the pathogenesis of asthma.....</b>  | <b>28</b> |
| <b>Table 2. Statistical analysis of IL-5 concentration in BALF from select groups of OVA or vehicle sensitized mice after treatment with 50 mg/kg TCH-013, vehicle or 0.1 mg/kg dexamethasone.....</b>  | <b>30</b> |
| <b>Table 3. Statistical analysis of IL-13 concentration in BALF from select groups of OVA or vehicle sensitized mice after treatment with 50 mg/kg TCH-013, vehicle or 0.1 mg/kg dexamethasone.....</b> | <b>32</b> |
| <b>Table 4. Statistical analysis of IL-6 concentration in BALF from select groups of OVA or vehicle sensitized mice after treatment with 50 mg/kg TCH-013, vehicle or 0.1 mg/kg dexamethasone.....</b>  | <b>34</b> |
| <b>Table 5. Statistical analysis of KC concentration in BALF from select groups of OVA or vehicle sensitized mice after treatment with 50 mg/kg TCH-013, vehicle or 0.1 mg/kg dexamethasone.....</b>    | <b>36</b> |
| <b>Table 6. Inhibition of the chymotryptic-like activity of purified human 20S proteasome by compounds 11-33 .....</b>  | <b>41</b> |
| <b>Table 7. Inhibition of the chymotryptic-like activity of purified human 20S proteasome by compounds 34-46 .....</b>  | <b>43</b> |

## LIST OF FIGURES

|   |    |
|---|----|
| Figure 1. Chemical structures of the proteasome inhibitors TCH-013 and bortezomib .....   | 7  |
| Figure 2. The classical and alternative pathways of NF- $\kappa$ B.....   | 8  |
| Figure 3. Serum concentrations of TCH-013 in BALB/c mice at 1, 3, and 12 hours after IP administration of drug at 150 mg/kg .....                           | 21 |
| Figure 4. TCH-013 reduces LPS-induced TNF- $\alpha$ production .....  | 22 |
| Figure 5. Total cell counts in BALF from OVA or vehicle sensitized mice after treatment with 50 mg/g TCH-013, saline or 0.1 mg/kg dexamethasone.....        | 23 |
| Figure 6. Eosinophil count in BALF from OVA or vehicle sensitized mice after treatment with 50mg/kg TCH-013, saline or 0.1mg/kg dexamethasone.....          | 24 |
| Figure 7. Lymphocyte count in BALF from OVA or vehicle sensitized mice after treatment with TCH-013, saline or dexamethasone.....                           | 25 |
| Figure 8. Neutrophil count in BALF from OVA or vehicle sensitized mice after treatment with 50 mg/kg TCH-013, saline or 0.1 mg/kg dexamethasone.....        | 26 |
| Figure 9. Monocyte count in BALF from OVA or vehicle sensitized mice after treatment with 50 mg/kg TCH-013, saline or 0.1 mg/kg dexamethasone.....          | 27 |
| Figure 10. IL-5 concentration in BALF from OVA or vehicle sensitized mice after treatment with 50 mg/kg TCH-013, vehicle or 0.1 mg/kg dexamethasone.....    | 29 |
| Figure 11. IL-13 concentration in BALF from OVA or vehicle sensitized mice after treatment with TCH-013, vehicle or dexamethasone.....                      | 31 |
| Figure 12. IL-6 concentration in BALF from OVA or vehicle sensitized mice after treatment with TCH-013, vehicle or dexamethasone.....                       | 33 |
| Figure 13. KC concentration in BALF from OVA or vehicle sensitized mice after treatment with TCH-013, vehicle or dexamethasone.....                         | 35 |
| Figure 14. Total lung resistance after methacholine challenge in OVA or vehicle sensitized mice after treatment with TCH-013, saline or dexamethasone ..... | 37 |
| Figure 15. Dose response curve showing the change in velocity of Suc-LLVY-AMC hydrolysis at variable concentrations of TCH-013 .....                        | 40 |

|   |           |
|---|-----------|
| <b>Figure 16. Kinetic analysis of CT-L activity inhibition by compound 43 .....</b>   | <b>44</b> |
| <b>Figure 17. Cell viability of THP-1 wild type cells after 72 hours of treatment with 10 <math>\mu</math>M imidazoline .....</b>                               | <b>47</b> |
| <b>Figure 18. Cell viability of THP-1 BTZ500 cells after 72 hours of treatment with 10 <math>\mu</math>M imidazoline or 1 <math>\mu</math>M bortezomib.....</b> | <b>48</b> |
| <b>Figure 19. Compound 43 is present in the serum after IP administration at 150 mg/kg.....</b>   | <b>51</b> |
| <b>Figure 20. Compound 43 reduces LPS-induced TNF-<math>\alpha</math> production. ....</b>  | <b>52</b> |

## KEY TO ABBREVIATIONS

|                  |  |
|------------------|--|
| AHR              | airway hyperresponsiveness                 |
| ALT              | alanine aminotransferase                   |
| AMC              | aminomethylcoumarin                        |
| ANOVA            | analysis of variance                       |
| BALF             | bronchoalveolar lavage fluid               |
| BBB              | blood brain barrier                        |
| BTZ500           | bortezomib resistant THP1 cells            |
| CO <sub>2</sub>  | carbon dioxide                             |
| D5W              | 5% dextrose in water                       |
| DILI             | drug induced liver injury                  |
| DMSO             | dimethylsulfoxide                          |
| ELISA            | enzyme linked immunosorbent assay          |
| FDA              | United States Food and Drug Administration |
| h                | hours                                      |
| IC <sub>50</sub> | inhibitory concentration 50%               |
| ICAM             | intracellular adhesion molecule            |
| Ig               | immunoglobulin                             |
| IFN              | interferon                                 |
| IκB              | inhibitor of kappa B                       |
| IκK              | inhibitor of kappa kinase                  |
| IL               | interleukin                                |
| IP               | intra-peritoneal                           |

|                |   |
|----------------|---|
| KC             | keratinocyte chemoattractant            |
| $K_M$          | Michaelis constant                      |
| LC/MS          | liquid chromatography/mass spectrometry |
| LPS            | lipopolysaccharide                      |
| MCL            | mantle cell lymphoma                    |
| MM             | multiple myeloma                        |
| NF- $\kappa$ B | nuclear factor kappa B                  |
| OVA            | ovalbumin                               |
| RA             | rheumatoid arthritis                    |
| S              | svedberg unit                           |
| [S]            | substrate concentration                 |
| SEM            | standard error of the mean              |
| TNF- $\alpha$  | tumor necrosis factor alpha             |
| VCAM           | vascular cell adhesion molecule         |
| $V_{max}$      | maximum velocity                        |
| WT             | wild type                               |

## CHAPTER 1- INTRODUCTION

### The ubiquitin-proteasome system

A key component of biological homeostasis is the targeted degradation of intracellular proteins by the ubiquitin-proteasome system.<sup>1</sup> Mutated and misfolded proteins, as well as those involved in inflammation, gene expression, and cell division are just a few examples of proteins regulated by this degradation mechanism.<sup>2,3</sup>

The human proteasome is a multi-subunit protein complex responsible for the regulation of protein homeostasis through degradation.<sup>4</sup> The barrel-like structure of the 26S proteasome consists of two 19S regulatory caps that flank four stacked rings of the 20S catalytic core. The 19S cap is a six membered ring consisting of AAA-ATPases that are responsible for unfolding and recognizing ubiquitinated proteins.<sup>5</sup> These processed proteins are then shuttled into the center of the 20S catalytic core. The outermost parts of the 20S unit are composed of the seven membered  $\alpha$ -rings, which are responsible for interaction with the 19S regulatory caps. The center of the barrel-like structure is formed by two  $\beta$ -rings that consist of seven subunits each, three of which are responsible for proteolysis.<sup>6</sup> The unfolded proteins encounter a catalytic threonine on the  $\beta$ 1,  $\beta$ 2, or  $\beta$ 5 subunit where they undergo an amide cleavage reaction and are broken down.<sup>7</sup> Each of these subunits has a unique cleavage profile, the  $\beta$ 1 has caspase-like activity, the  $\beta$ 2 has trypsin-like activity and the  $\beta$ 5 has chymotrypsin-like activity. Disruption of the peptidase activity of these subunits is the target of proteasome inhibition.<sup>8,9</sup>

In 2003, the FDA approved bortezomib, the first in class proteasome inhibitor shown in Figure 1, for the treatment of multiple myeloma (MM). Since that time, bortezomib has been approved for the treatment of refractory mantle cell lymphoma (MCL) and second generation proteasome inhibitors have been developed as treatments for malignancies and auto-immune disorders.<sup>10,11</sup> Unfortunately, there are several drawbacks to bortezomib therapy, including dose-limiting peripheral neuropathy, limited activity in solid tumors, resistance and route of administration restrictions.<sup>12,13</sup> It has been suggested that alteration of the pharmacokinetics and pharmacodynamics of proteasome inhibitors will alleviate the restrictions of bortezomib therapy.<sup>14,15</sup>

The keystone of the mechanism of bortezomib therapy is the role the proteasome plays in NF- $\kappa$ B activation.<sup>16,17</sup> Although NF- $\kappa$ B activation can be initiated through two different pathways, classical and alternative, a common event in these signaling cascades is the proteasomal degradation of inhibitory proteins (Figure 2).<sup>18,19</sup> Activation of NF- $\kappa$ B has been implicated as a significant promoter of pro-survival/pro-inflammatory signaling in many different types of cancers and autoimmune diseases.<sup>20,21</sup>

In the classical pathway, illustrated on the left portion of Figure 2, the active components of NF- $\kappa$ B exist as a complex with an inhibitory protein, I $\kappa$ B $\alpha$ . Upon response to the principal activators, LPS, IL-1, or TNF- $\alpha$ , I $\kappa$ K $\beta$  is activated and phosphorylates I $\kappa$ B $\alpha$  which leads to ubiquitination, marking it for proteasomal degradation.<sup>22,23</sup> When the NF- $\kappa$ B complex encounters the proteasome, the I $\kappa$ B

protein is degraded, liberating the active subunits (p65/p50), which then translocate into the nucleus and initiate transcription of NF- $\kappa$ B mediated genes responsible for innate immunity, cell survival, and inflammation.<sup>24</sup>

The alternative pathway, shown on the right side of Figure 2, which mediates adaptive immunity and lymphoid development, follows a similar pathway. Activation of the CD40, LT- $\beta$ , or BAFF receptors activates I $\kappa$ K $\alpha$  which phosphorylates p100. The ubiquitination and processing of p100 follows, resulting in translocation of p52/RelB into the nucleus and subsequent transcription of target genes.<sup>22</sup>

The impact of proteasome inhibition on NF- $\kappa$ B signaling results in both anti-inflammatory and anti-proliferative effects.<sup>9</sup> As of 2010, all clinically evaluated proteasome inhibitors exhibited a competitive mechanism of action via irreversible covalent binding to the catalytic threonine of the  $\beta$ 5 subunit.<sup>25,26</sup> This binding profile results in toxic accumulation of intracellular proteins and disruption of NF- $\kappa$ B activation in both healthy and malignant cells.<sup>17</sup>

### **Identification of the imidazoline scaffold as an inhibitor of NF- $\kappa$ B through modulation of the proteasome**

In 2004, the same year that Aaron Ciechanover, Avram Hersheko and Irwin Rose were awarded the Nobel Prize for their discovery of the proteasome, the Tepe laboratory identified the molecule TCH-013 as a potent inhibitor of NF- $\kappa$ B signaling (Figure 1).<sup>27,28</sup> Subsequent studies involving this molecule, including kinetic analysis



and evaluation of bortezomib cross-resistance, identified the mechanism of action as noncompetitive proteasome inhibition.<sup>28,29</sup>

The unique mechanism of action has attractive therapeutic potential for autoimmune and malignant diseases. Models of rheumatoid arthritis (RA) and MM in a xenograft setting were employed to evaluate the effectiveness of this molecule *in vivo*.<sup>29,30</sup> In cell culture, TCH-013 was found to induce apoptosis in MM cells, but exhibited limited cytotoxicity against primary bone marrow stromal cells.<sup>29</sup> Encouraging results, such as reduced tumor burden and RA disease score, showed efficacy against both disease states. In addition to inhibiting disease progression, treatment exhibited limited toxicity, observed as no apparent weight loss or increase in serum alanine aminotransferase (ALT).<sup>30</sup> These studies indicate that a noncompetitive proteasome inhibitor is effective in animal models with limited toxicity and have opened a window for the development of more potent analogs of these molecules and application to other diseases.

### **The role of NF- $\kappa$ B in asthma and the proteasome inhibitor as potential steroid sparing therapy**

Asthma, a disease characterized by wheezing, coughing, and shortness of breath, affected over 24 million Americans in 2009.<sup>31</sup> Steroids remain the primary therapy for the treatment of this disease; however, the extensive side effects associated with these drugs (weight gain, indigestion, osteoporosis, and glucose intolerance) have encouraged the medical community to search for adjunctive or alternative

therapies.<sup>32,33</sup> NF- $\kappa$ B has emerged as an attractive therapeutic target for the treatment of asthma, due to the regulation of many important immunomodulatory and proinflammatory genes involved in the pathogenesis of the disease.<sup>34,35</sup> Of particular importance is the role of NF- $\kappa$ B in the recruitment and activation of eosinophils, a process which has been identified as an important early in the development of asthma.<sup>36</sup>

Attenuation of NF- $\kappa$ B in allergic airway disease has been achieved with mixed results by administration of proteasome inhibitors, oligonucleotides, mutation of I $\kappa$ B $\alpha$ , and mutation of I $\kappa$ K.<sup>33,37</sup> Interestingly, administration of a proteasome inhibitor significantly reduced pulmonary eosinophilia but did not appear to disrupt airway remodeling or hyperresponsiveness.<sup>38,39</sup>

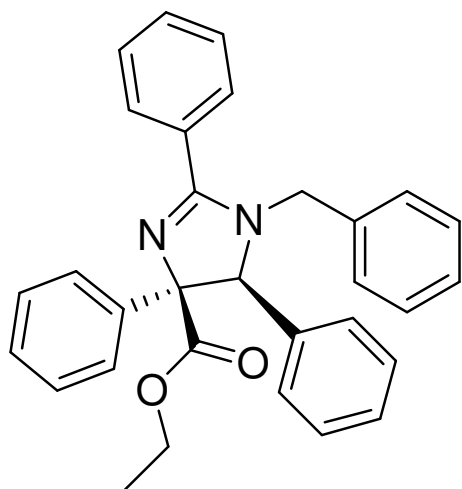
### **Disruption of NF- $\kappa$ B signaling through proteasome inhibitors as treatment for multiple myeloma**

In 2009, approximately 20,500 individuals were diagnosed with multiple myeloma, a plasma cell neoplasm with a five year relative survival rate of only 35% and a sustained remission rate of 3%.<sup>40,41</sup> NF- $\kappa$ B, which is dysregulated in MM, controls transcription of many of the key pathogenetic factors, including IL-6, ICAM-1, VCAM-1.<sup>18,42</sup> Inhibition of the NF- $\kappa$ B pathway, and these mediators, has been achieved by the aforementioned proteasome inhibitor bortezomib.<sup>43,44</sup> Despite successful disruption of the NF- $\kappa$ B pathway and amelioration of disease pathogenesis, bortezomib

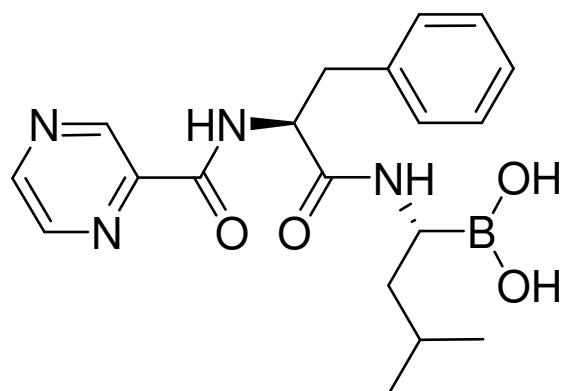
has limited clinical potential due to its narrow therapeutic window, the development of resistance mechanisms and limited bioavailability.<sup>12,45</sup>

The chronic treatment of the human leukemia cell line, THP-1, with bortezomib lead to development of a proteasome inhibitor resistant strain.<sup>46</sup> A mutation in the binding site of bortezomib and overexpression of the  $\beta 5$  subunit was identified through genetic and proteomic analysis to be the mechanism for developed resistance.<sup>47</sup> Recent studies indicate that noncompetitive proteasome inhibitors are able to overcome resistance by circumventing direct interaction with the mutated and overexpressed  $\beta 5$  subunit.<sup>25,29</sup>

The development of non-toxic proteasome inhibitors for the treatment of malignancies and autoimmune disorders is crucial. The data presented herein suggests that a modified imidazoline scaffold is an effective and non-toxic proteasome inhibitor that can overcome bortezomib resistance and has therapeutic potential for the treatment of multiple myeloma and inflammatory conditions.



**TCH-013**



**bortezomib**

**Figure 1. Chemical structures of the proteasome inhibitors TCH-013 and bortezomib.**

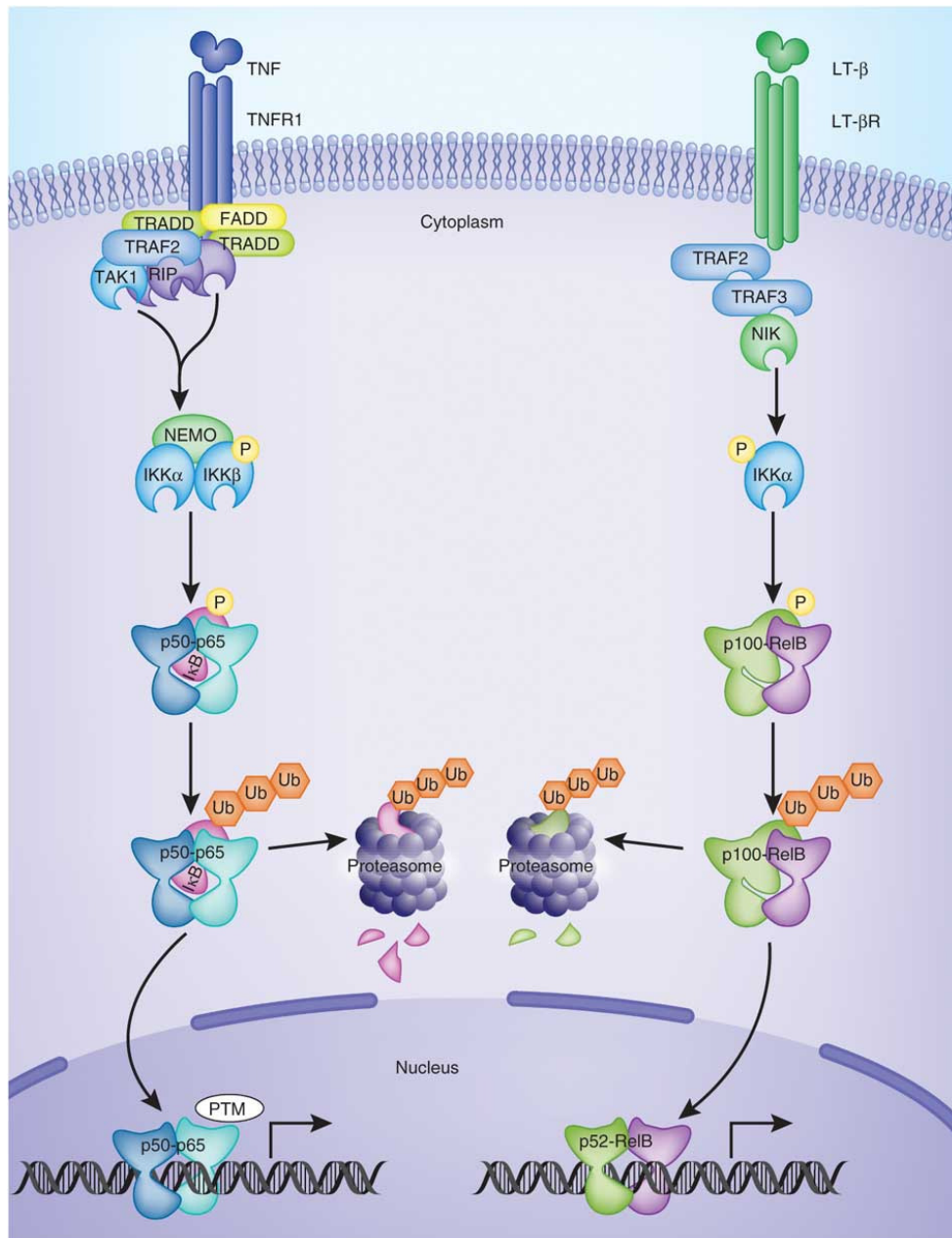


**Figure 2. The classical and alternative pathways of NF-κB.** Under normal conditions, NF-κB is bound to the IκB inhibitory proteins in the cell cytoplasm. Extracellular signals begin the activation process by inducing phosphorylation of IκB. The phosphorylated IκB proteins are then ubiquitinated and subsequently degraded by the proteasome. This process releases the active NF-κB which then translocates into the nucleus. The classical activation pathway, on the left of this figure, is represented with TNF signaling. The alternative pathway, on the right of this figure, is represented with LT-β signaling. Reprinted by permission from Macmillan Publishers Ltd: *NATURE IMMUNOLOGY*, copyright 2011.<sup>48</sup>

## **CHAPTER 2- MATERIALS AND METHODS**

### **Reagents**

Bortezomib was purchased from Selleck Biochemicals (Houston, TX), fluorogenic substrates and purified proteasome particles from Boston Biochem (Cambridge, MA). All antibodies were purchased from Santa Cruz Biotechnologies (Santa Cruz, CA) or Cell Signaling Technology (Danvers, MA) and ELISA kits from R&D Systems (Minneapolis, MN). Cell culture media and supplements were purchased from Life Technologies (Grand Island, NY), all other chemicals were purchased from Sigma-Aldrich (St. Louis, MO).

### **Cell culture**

The human cell line RPMI-8226 was purchased from American Type Culture Collection (Manassas, VA); THP-1 and THP-1/BTZ500 were a kind gift from Dr. Oerlemans of the VU University Medical Center, Amsterdam, The Netherlands.<sup>47</sup> Cell lines were maintained in RPMI-1640 media supplemented with 10% fetal bovine serum, 100 U/mL penicillin, 100 mg/mL streptomycin, 1 mM sodium pyruvate, and 0.2 mM L-glutamine. Cells were cultured at 37 °C, 5% CO<sub>2</sub>.

### **Animals and husbandry**

Female, immune competent BALB/c mice were bred in the McCormick laboratory at Michigan State University or purchased from Charles River (Wilmington, MA). The animals were given access to water and food (Teklad 7904) *ad libitum* and were

maintained in a pathogen free environment. Animal rooms were maintained at 21-24° C with 40-55% relative humidity, and were set on a 12 hour light/dark cycle. All procedures involving animals were performed with approval from the Michigan State University Institutional Animal Care and Use Committee in accordance with all policies and guidelines.

### **OVA-induced allergic airway model**

Induction of allergic airway disease was achieved as previously described.<sup>49</sup> In short, mice were randomly assigned to either vehicle or OVA treatment groups. The vehicle group received an IP injection of 250 µL saline, while the OVA group received OVA/alum (20 µg/1 mg in 250 µL saline). Ten days after sensitization, OVA animals were injected with a boost of OVA (20 µg in 250 µl saline) and vehicle animals received saline alone. One week following the boost, animals were challenged with OVA or saline via inhalation for three consecutive days. Animals were administered vehicle (30:70 propylene glycol:D5W), TCH-013 (50 mg/kg), or dexamethasone (0.1 mg/kg), one hour prior to each nebulizer challenge. Pentobarbital sodium (50 mg/kg) was used to anesthetize mice 48 hours after final challenge, after which a midline laparotomy was performed. Bronchoalveolar lavage fluid (BALF) was collected and analyzed for total and differential cell counts using a hemacytometer and Diff-Quick reagent (Baxter, Deerfield, IL).

## **Pulmonary function analysis**

Mice were anesthetized with an IP injection of pentobarbital sodium (50 mg/kg) after which time they were subsequently intubated, and ventilated with a small animal ventilator (SAV, *flexiVent*; SCIREQ, Montreal, Quebec, Canada). Ventilator settings were set at an initial frequency of 120–150 respirations/minute and at a volume of 1.5 mL/kg. An Aeroneb nebulizer (Aerogen) was used to administer variable doses of methacholine, and *flexiVent* pulmonary function testing system was used to measure total lung resistance (SnapShot-150; SCIREQ). Following data collection, the mice were euthanized and BALF was collected as described above.

## **Cytokine bead array**

Cytokine content of BALF was analyzed using Cytometric Bead Array kits and reagents (BD Bioscience, Franklin Lakes, NJ) according to manufacturer's suggested protocol. In brief, BALF samples are analyzed using a flow cytometer after they have been mixed with the cytokine-specific antibody coated beads. The presence of specific cytokines is based on the specific fluorescent signature of each bead. Samples supplied by the manufacturer were used to calculate standard curves for each cytokine.

## **Enzymatic activity assessment**

The fluorogenic substrate Suc-LLVY-AMC was used to measure chymotryptic-like proteasome activities using 1 nM purified 20S proteasome.<sup>50</sup> The rate of cleavage of fluorogenic peptide substrates was determined by monitoring the fluorescence of released aminomethylcoumarin (AMC) using a SpectraMax M5e multiwell plate reader



at an excitation wavelength of 380 nm and emission wavelength of 460 nm. Fluorescence was measured at 37 °C every minute over a 30 minute period and the maximum increase in fluorescence per minute was used to calculate specific activities of each sample. IC<sub>50</sub> was calculated by non-linear regression analysis using GraphPad prism software (La Jolla, CA).  $K_M$ , and  $V_{max}$  values were calculated from Michaelis–Menten analysis using variable concentrations of Suc-LLVY-AMC and imidazoline.

### **Cytotoxicity measurement**

Cell viability was assayed 72 hours after drug treatment using the CellTiter 96® AQueous One Solution Cell Proliferation Assay (Promega Corporation, Madison WI) according to manufacturer specifications. Drugs were dissolved in DMSO and added to cell culture to reach a final concentration of 10 µM or 5 µM drug and 0.5% DMSO. The absorbance of formazan was measured at 490 nm on a SpectraMaxM5e microplate reader. Background absorbance was subtracted from each measurement and viability was calculated using the vehicle control as 100%. Drug potency was expressed as IC<sub>50</sub> and was calculated by non-linear regression analysis using GraphPad prism software (La Jolla, CA).

### **Development of bortezomib resistant cell lines**

The human cell line THP-1 cells were a kind gift from Dr. Oerlemans of the VU University Medical Center, Amsterdam, The Netherlands. Cells were maintained in

RPML-1640 media supplemented with 10% fetal bovine serum, 100 U/mL penicillin, 100 mg/mL streptomycin, 1 mM sodium pyruvate, and 0.2 mM L-glutamine. Cells were cultured at 37° C, 5% CO<sub>2</sub>. BTZ500 cells were maintained in complete media with 500 nM bortezomib and were given a 72 hours washout period before the cell viability assay. Drugs were dissolved in DMSO and added to cells to reach a final concentration of 10 µM drug and 0.5% DMSO. Cytotoxicity was assayed after 72 hours as described above.

### **Bioavailability**

To determine bioavailability of the compounds, liquid crystal mass spectroscopy (LC/MS) was performed on serum samples as previously described.<sup>29</sup> In short: female, BALB/c mice received 50 mg/kg of drug in 30% propylene glycol: D5W via intraperitoneal injection. Blood was drawn via saphenous vein collection into 75mm hematocrit tubes (Drummond; Broomall, PA) at 1, 3, and 6 hours post imidazoline injection. Isolated serum was processed and supernatant was transferred to a polypropylene microplate. LC/MS analysis to determine drug concentration was performed in the MSU Mass Spectrometry Core under the direction of Dr. Dan Jones using a Waters LCT Premier mass spectrometer in conjunction with a Waters Atlantis dC18 column. Positive mode electrospray ionization was used to analyze supernatant volumes injected in concentrations of 10 µL. Purified drug standards were analyzed to determine retention times and response factors.

### **ALT assay**

To assess hepatotoxicity, serum was collected from animals treated with an extended dosing regimen of TCH-013 to assess hepatotoxicity after subacute exposure (13-19 days). Animals were treated with vehicle or TCH-013 (50 mg/Kg and 150 mg/Kg) via intraperitoneal injection. Drug was administered on days 1-5, 8-12, and 15-19; on days 6-7, and 13-14 animals were not treated. The animals were sacrificed when distress was observed by laboratory staff according to IACUC guidelines; length of treatment ranged from 13-19 days. Blood was collected via cardiac puncture and serum samples were analyzed for ALT according to manufacturer specifications using Infinity™ ALT reagent (Thermo Fisher Scientific, Middletown, VA).

### **LPS challenge**

Immune competent BALB/c mice were treated with one IP injection of TCH-013 (50 mg/kg in 30:70 propylene glycol:D5W) 1 hour prior to dosing with 1 mg/kg LPS (E.coli -055B5). Animals were sacrificed 2 hours after LPS administration and blood was collected by cardiac puncture. Serum was collected and analyzed for TNF- $\alpha$  using an ELISA procedure.

### **ELISA**

The presence of TNF- $\alpha$  in serum was assessed using the commercially available mouse TNF- $\alpha$  Quantikine ELISA Kit (R&D Systems, Minneapolis, MN). ELISA was performed according to manufacturer specifications. Blood was collected as described above following LPS challenge protocol.

## **Statistical analysis**

Statistical analysis was performed using GraphPad Prism for Windows, GraphPad Software, San Diego California USA, [www.graphpad.com](http://www.graphpad.com).

All data are presented as mean  $\pm$  standard error of the mean (SEM). For the comparison of two groups, statistical significance was defined by a *p* value of 0.05 or less as determined by Student's *t* test. A one-way ANOVA with post-hoc analysis using Tukey's multiple comparison test was used to determine the significance between multiple groups unless otherwise noted.

## CHAPTER 3- RESULTS AND DISCUSSION

### **TCH-013 is bioavailable, non-toxic and disrupts the inflammatory cellular profile of BALF but not airway hyperresponsiveness in an experimental model of asthma**

Prior to evaluation in an animal model of experimental asthma, TCH-013 was evaluated for bioavailability and toxicity *in vivo*. Immune competent BALB/c mice were treated with a single dose of TCH-013 (150 mg/kg), administered intraperitoneally, in a vehicle comprised of 30:70 propylene glycol:D5W. Serial blood draws at 1, 3, and 12 hours were performed to determine the level of TCH-013 in the serum after dosing. Figure 3 represents LC/MS analysis of the serum obtained; indicating that IP administration of the compound produces blood levels in the micromolar range ( $n > 3$ ). Studies to determine organ distribution, blood brain barrier (BBB) permeability, metabolism, and elimination characteristics are needed to further investigate the pharmacokinetic properties of TCH-013.

Although no significant weight loss was reported with administration of TCH-013, further assessment of the compounds toxicity was warranted.<sup>30</sup> Discontinuation of candidate during the drug development process is most commonly caused by drug induced liver injury (DILI).<sup>51</sup> The standard biomarker used to monitor DILI, alanine aminotransferase (ALT), was measured in animals receiving IP TCH-013 at either 50 mg/kg (BID for 19 days) or 150 mg/kg (BID for 13 days) to assess the compounds liver toxicity.<sup>30,51</sup> These studies found no significant increase in serum ALT between the treatment groups and the vehicle groups ( $p > 0.05$ ,  $n \geq 4$ ) indicating TCH-013 is not hepatotoxic, as measured by serum ALT. Further studies including liver histology,

organ function, and evaluation of carcinogenesis are necessary to conclude that this compound has a clinically acceptable toxicity profile.

The inflammatory cytokine, TNF- $\alpha$ , has been implicated as an important mediator in the pathogenesis of asthma.<sup>52</sup> In order to determine if TCH-013 could ameliorate inflammatory response *in vivo* and if there was indication for application in the treatment of asthma, a lipopolysaccharide (LPS) model of systemic inflammation monitored by serum TNF- $\alpha$  was employed. LPS has been used previously to produce a robust inflammatory response that can be monitored by serum TNF- $\alpha$ .<sup>30</sup> Immune competent BALB/c mice were treated with an IP injection of 50 mg/kg TCH-013 one hour prior to administration of 1 mg/kg LPS. Two hours after LPS administration, animals were sacrificed and serum was collected. Figure 4 illustrates that TCH-013 significantly reduced serum TNF- $\alpha$  in response to LPS when measured by ELISA ( $p < 0.05$ ,  $n > 4$ ). TCH-013 was found, through LC/MS analysis, to be present in the serum of these animals in concentrations of  $4.6 \pm 1.0 \mu\text{M}$ . The results of this study indicate that these compounds have *in vivo* efficacy against systemic inflammation and thus may be useful in an experimental model of asthma.

Cellular infiltrate and resultant cellular response are considered chief mediators in the pathogenesis of asthma, their unique roles are outlined in Table 1<sup>53-55</sup>. Analysis of the bronchoalveolar lavage fluid (BALF) indicates that treatment with TCH-013 decreases the presence of inflammatory cells. BALF was collected immediately following the flexi-vent procedure 48 hours after the last OVA or saline challenge and total and differential cell counts were obtained. Figures 5-9 illustrate that OVA sensitized mice treated with vehicle exhibited a significant increase in total cells,

eosinophils, neutrophils and lymphocytes, when compared to vehicle control ( $p < 0.05$ ,  $n \geq 5$ ). Dexamethasone significantly attenuated this response in total cells and in all of the inflammatory cell types, and TCH-013 reduces the BALF concentrations of total cells, macrophages, eosinophils and lymphocytes (Figures 5-9,  $p < 0.05$ ,  $n \geq 5$ ). Since eosinophils are considered a hallmark of allergic airway disease by causing epithelial damage and airway hyperresponsiveness (AHR), the attenuation of their response indicates potential clinical application for these compounds.<sup>53,54</sup>

In addition to inflammatory cell quantification, cytokine evaluation of the BALF was also employed. Cytokines are secreted proteins that are responsible for many components of the immune response, especially cell trafficking and activation<sup>56</sup>. Inflammatory cytokines important to the pathogenesis of asthma were measured in the BALF using the BD Cytometric Bead Array (CBA).<sup>57</sup> IL-4, IFN- $\gamma$ , and TNF- $\alpha$  were measured but were below the limit of detection. Figures 10-13 show that ovalbumin sensitization induced a significant increase in IL-5, IL-6, IL-13 and KC in the vehicle treated animals ( $p > 0.05$ ,  $n \geq 7$ ). Neither TCH-013 nor dexamethasone treatment significantly reduced BALF cytokine levels. A complex statistical analysis was completed on these samples using ANOVA with Bonferroni's multiple comparison test, ANOVA with Tukey's multiple comparison test, and with Student's t-test (Tables 2-5). A plausible explanation for the apparent disconnect between the BALF cellular profile and the BALF cytokine profile, is the time point at which the BALF was taken. At 48 hours after final ovalbumin challenge, many of the cytokines will be well beyond their peak response, measurements of these cytokines at various time points would yield a better

picture of the cytokine profiles.<sup>58</sup> These studies did not evaluate the presence of cells in the lung parenchyma; if their properties and numbers were not affected by the drug treatments, they could be responsible for secreting cytokines as well.

To assess the effect of TCH-013 on airway hyperresponsiveness, mice were mechanically ventilated 48 hours after final OVA challenge and total lung resistance was measured. Ovalbumin sensitized mice treated with vehicle exhibited airway hyperresponsiveness characterized by an increase in total lung resistance after treatment with methacholine ( $p < 0.05$ ,  $n \geq 5$ ). Treatment with TCH-013 or dexamethasone did not significantly affect airway hyperresponsiveness in ovalbumin sensitized mice or in the control mice (Figure 14). This result was unexpected because of the robust decrease in inflammatory cells found in the BALF. There has been some debate in the literature about the relationship between NF- $\kappa$ B to the cellularity of the lavage fluid and airway remodeling in asthma.<sup>33,37</sup> In previous studies with TCH-013, it was shown that the compound lacks cytotoxic activity against bone marrow stromal cells.<sup>29</sup> It is possible that the inflammatory cells retained their ability to induce AHR and that the decreased number of cells was enough to initiate the pathogenic process.

Co-treatment with TCH-013 and a steroid, such as dexamethasone, would be necessary to determine if these proteasome inhibitors could be used as an adjunctive steroid sparing therapy. A more thorough analysis with particular attention paid to the relationship of the inflammation and pathogenesis to NF- $\kappa$ B inhibition via the proteasome is needed to determine the clinical potential for the imidazolines in allergic airway disease.



More recent studies involving bortezomib in an experimental model of asthma exhibited similar results to our studies, showing a decrease in cellularity without resultant changes in airway remodeling. These studies focused on the plasma cell depleting and IgE modulating effects of bortezomib.<sup>38</sup> In future studies involving TCH-013, these factors should be monitored so that the proteasome inhibitors can be compared across studies.

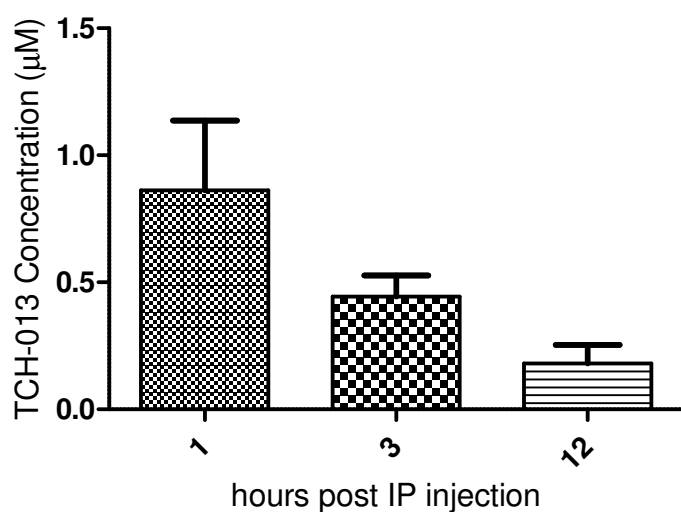


**Figure 3. Serum concentrations of TCH-013 in BALB/c mice at 1, 3, and 12 hours after IP administration of drug at 150 mg/kg (n >3).** Animals were given a single IP dose of TCH-013 in 30:70 propylene glycol:D5W and blood was drawn at 1, 3, and 12 hours post administration. LC/MS analysis was performed on the samples to determine the quantity of drug present.

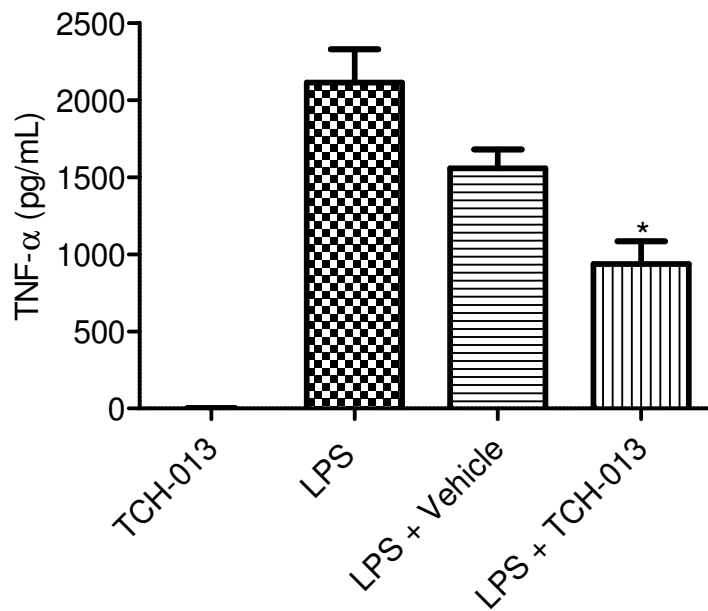


**Figure 4. TCH-013 reduces LPS-induced TNF- $\alpha$  production.** Animals were given an IP dose of 50 mg/kg TCH-013, followed one hour later by an IP dose of 1 mg/kg LPS, and two hours later serum was collected. Concentration of TNF- $\alpha$  in serum was measured using an ELISA. Serum concentrations of TNF- $\alpha$  after LPS challenge were significantly reduced by 50mg/kg IP dose of TCH-013 when compared to LPS + vehicle ( $p < 0.05$ ,  $n = 5$ ).

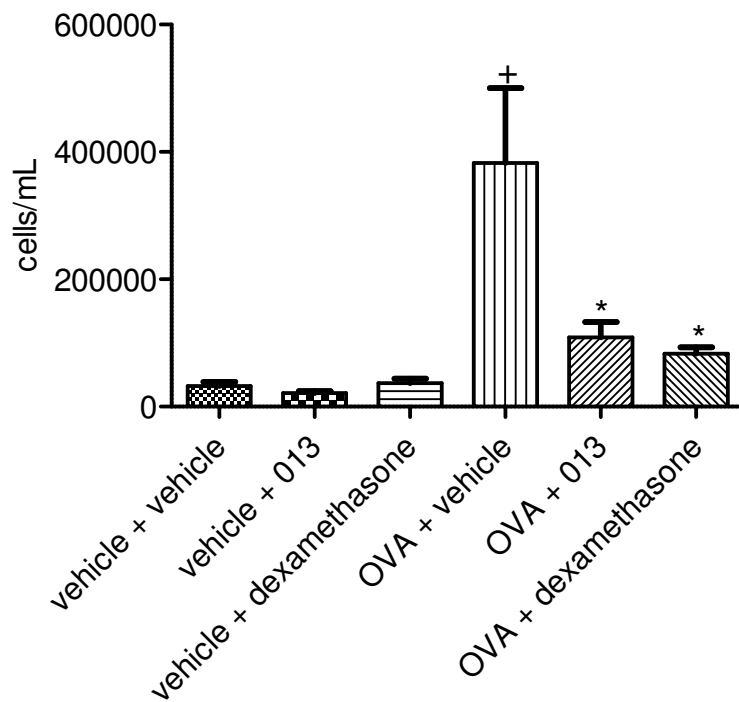


**Figure 5. Total cell counts in BALF from OVA or vehicle sensitized mice after treatment with 50 mg/g TCH-013, saline or 0.1 mg/kg dexamethasone.** Treatment with OVA induced a robust and statistically significant increase in total cells (+ $p < 0.05$ ,  $n = 8$ ). In OVA sensitized mice, treatment with TCH-013 or dexamethasone significantly reduced total cellularity of BALF when compared to vehicle (\* $p < 0.05$ ,  $n \geq 7$ ).

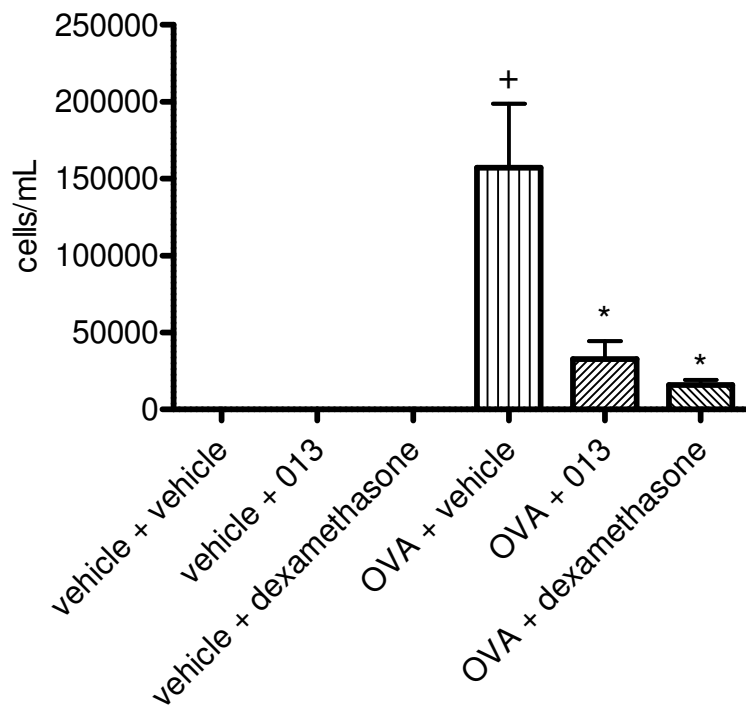


**Figure 6. Eosinophil count in BALF from OVA or vehicle sensitized mice after treatment with 50mg/kg TCH-013, saline or 0.1mg/kg dexamethasone.** Treatment with OVA induced a robust and statistically significant increase in total cells (+ $p < 0.05$ ,  $n = 7$ ). In OVA sensitized mice, treatment with TCH-013 or dexamethasone significantly reduced eosinophilia of BALF when compared to vehicle (\* $p < 0.05$ ,  $n \geq 7$ ).

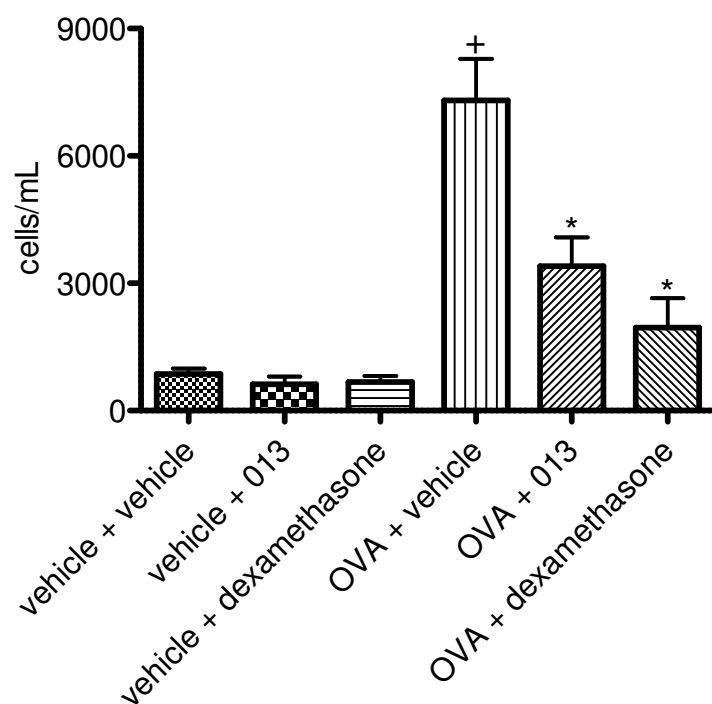


**Figure 7. Lymphocyte count in BALF from OVA or vehicle sensitized mice after treatment with 50 mg/kg TCH-013, saline or 0.1 mg/kg dexamethasone.** Treatment with OVA induced a robust and statistically significant increase in total cells ( $+p < 0.05$ ,  $n = 7$ ). In OVA sensitized mice, treatment with TCH-013 or dexamethasone significantly reduced lymphocytosis of BALF when compared to vehicle ( $*p < 0.05$ ,  $n \geq 6$ ).

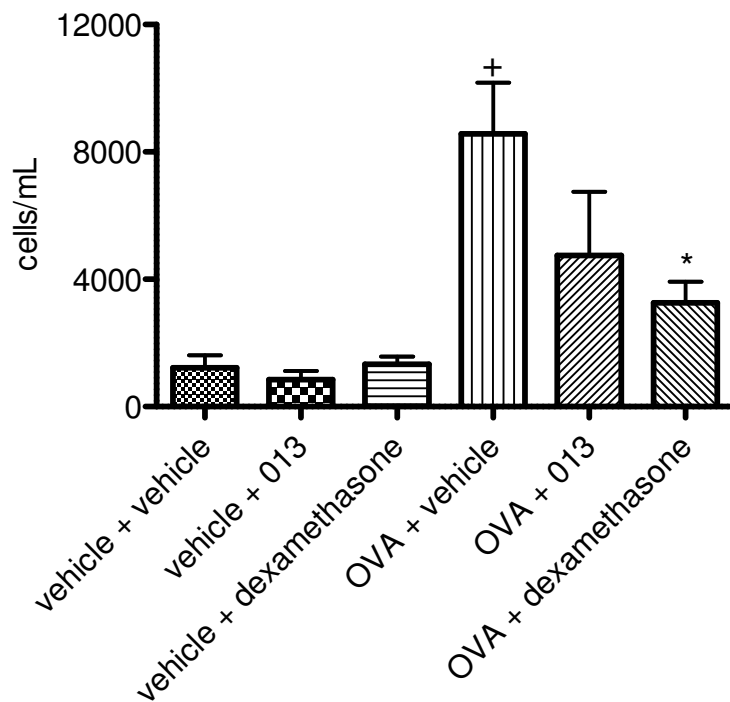


**Figure 8. Neutrophil count in BALF from OVA or vehicle sensitized mice after treatment with 50 mg/kg TCH-013, saline or 0.1 mg/kg dexamethasone.** Treatment with OVA induced a robust and statistically significant increase in total cells when compared to vehicle alone (+ $p < 0.05$ ,  $n = 7$ ). In OVA sensitized mice, treatment with TCH-013 or dexamethasone significantly reduced neutrophilia of BALF when compared to vehicle (\* $p < 0.05$ ,  $n \geq 6$ ).

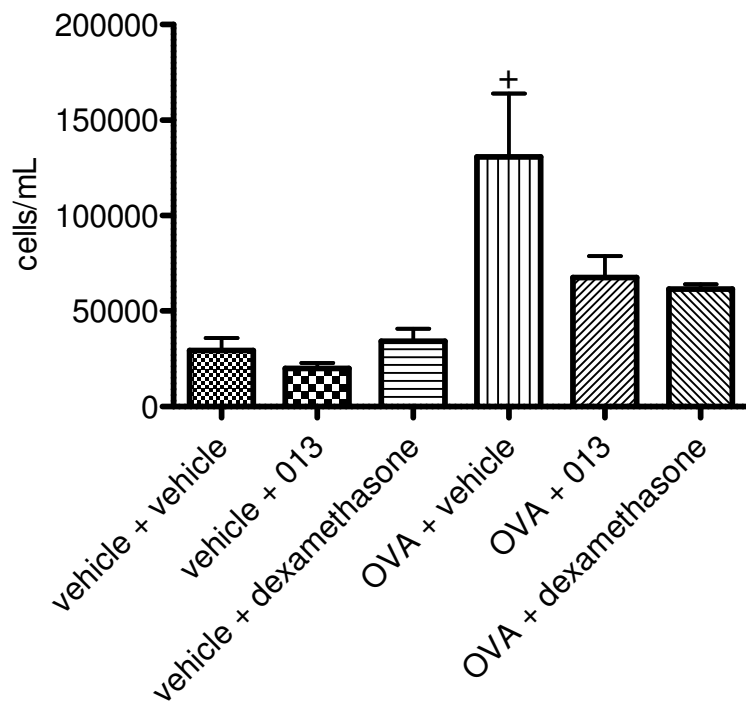


**Figure 9. Monocyte count in BALF from OVA or vehicle sensitized mice after treatment with 50 mg/kg TCH-013, saline or 0.1 mg/kg dexamethasone.** Treatment with OVA induced a robust and statistically significant increase in total cells (+ $p < 0.05$ ,  $n = 7$ ). There was not a significant decrease in the BALF monocytes of the OVA sensitized mice treated with TCH-013 or dexamethasone BALF when compared to vehicle ( $p > 0.05$ ,  $n \geq 5$ ).



| <b>Cytokine</b> | <b>Role</b>   |
|-----------------|---|
| IL-4            | Eosinophil growth<br>Increase TH <sub>2</sub> cells<br>Increase IgE                 |
| IL-5            | Eosinophil maturation<br>Inhibits apoptosis<br>Increase TH <sub>2</sub> cell<br>AHR |
| IL-6            | T and B Cell growth factor<br>Increase IgE  |
| IL-13           | Eosinophil activation<br>Inhibition of apoptosis<br>Increase IgE                    |
| IFN- $\gamma$   | Activate endothelial cells, epithelial cells, and macrophages                       |
| KC              | Recruitment of macrophages and neutrophils  |
| TNF- $\alpha$   | Activate epithelium, endothelium, APC, monocytes and macrophages<br>AHR             |

**Table 1. The role of cytokines in the pathogenesis of asthma.**

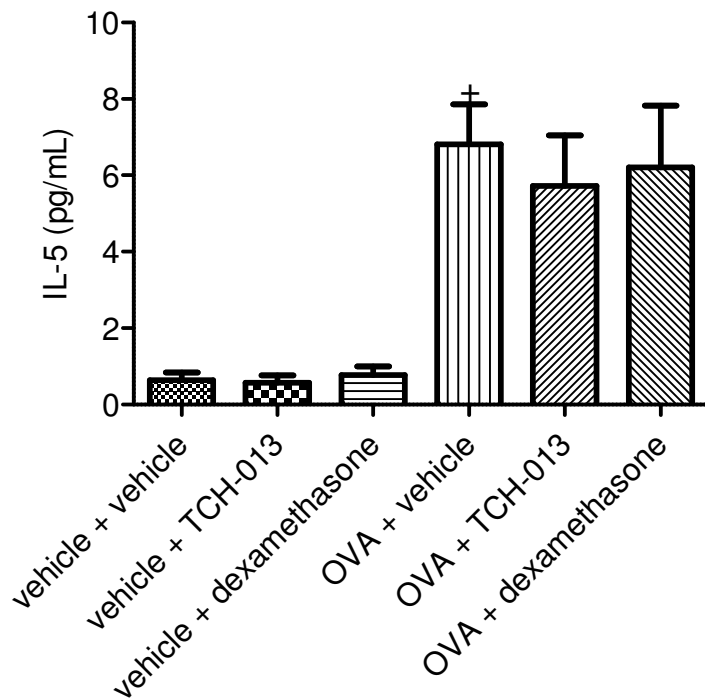


**Figure 10. IL-5 concentration in BALF from OVA or vehicle sensitized mice after treatment with 50 mg/kg TCH-013, vehicle or 0.1 mg/kg dexamethasone.** Treatment with OVA induced a statistically significant increase in IL-5 ( $+p < 0.05$ ,  $n \geq 8$ ). However, treatment with neither TCH-013 nor dexamethasone decreased IL-5 concentration in the BALF ( $p > 0.05$ ,  $n \geq 7$ ).

|                                       | <b>ANOVA with Bonferroni's multiple comparisons test, adjusted P value</b> | <b>ANOVA with Tukey's multiple comparisons test, adjusted P value</b> | <b>T test, P value</b> |
|---------------------------------------|--|---|------------------------|
| OVA + vehicle vs. OVA + TCH-013       | 0.9497   | 0.9497  | 0.5196                 |
| OVA + vehicle vs. OVA + dexamethasone | 0.9987   | 0.9987  | 0.7519                 |
| OVA + TCH-013 vs. OVA + dexamethasone | 0.9996   | 0.9996  | 0.8264                 |

**Table 2. Statistical analysis of IL-5 concentration in BALF from select groups of OVA or vehicle sensitized mice after treatment with 50 mg/kg TCH-013, vehicle or 0.1 mg/kg dexamethasone (n ≥ 7).**

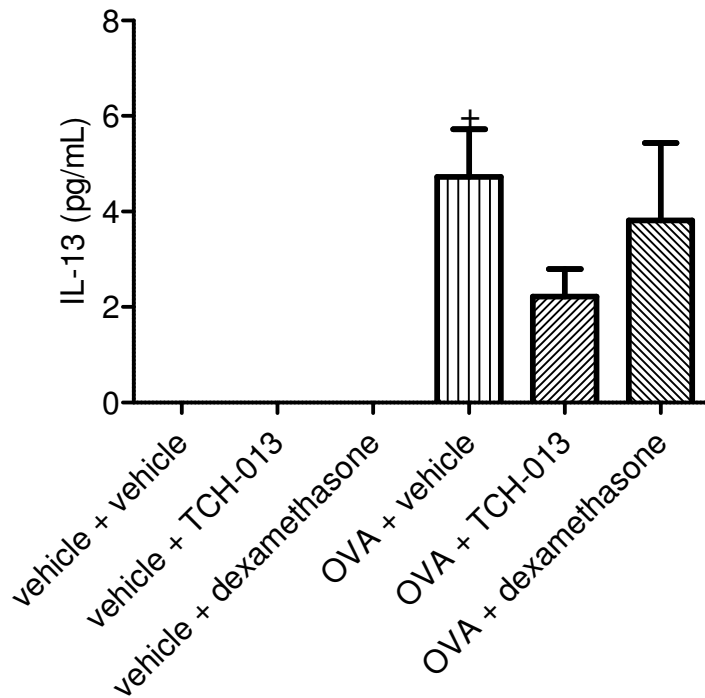


**Figure 11. IL-13 concentration in BALF from OVA or vehicle sensitized mice after treatment with 50 mg/kg TCH-013, vehicle or 0.1 mg/kg dexamethasone.** Treatment with OVA induced a statistically significant increase in IL-13 ( $p < 0.05$ ,  $n \geq 8$ ). However, treatment with neither TCH-013 nor dexamethasone decreased IL-13 concentration in the BALF ( $p > 0.05$ ,  $n \geq 7$ ).

|                                       | <b>ANOVA with Bonferroni's multiple comparisons test, adjusted P value</b> | <b>ANOVA with Tukey's multiple comparisons test, adjusted P value</b> | <b>T test</b> |
|---------------------------------------|--|---|---------------|
| OVA + vehicle vs. OVA + TCH-013       | 0.1478   | 0.0977  | 0.0456        |
| OVA + vehicle vs. OVA + dexamethasone | >0.9999  | 0.9700  | 0.6276        |
| OVA + TCH-013 vs. OVA + dexamethasone | >0.9999  | 0.7606  | 0.2652        |

**Table 3. Statistical analysis of IL-13 concentration in BALF from select groups of OVA or vehicle sensitized mice after treatment with 50 mg/kg TCH-013, vehicle or 0.1 mg/kg dexamethasone (n ≥ 7).**

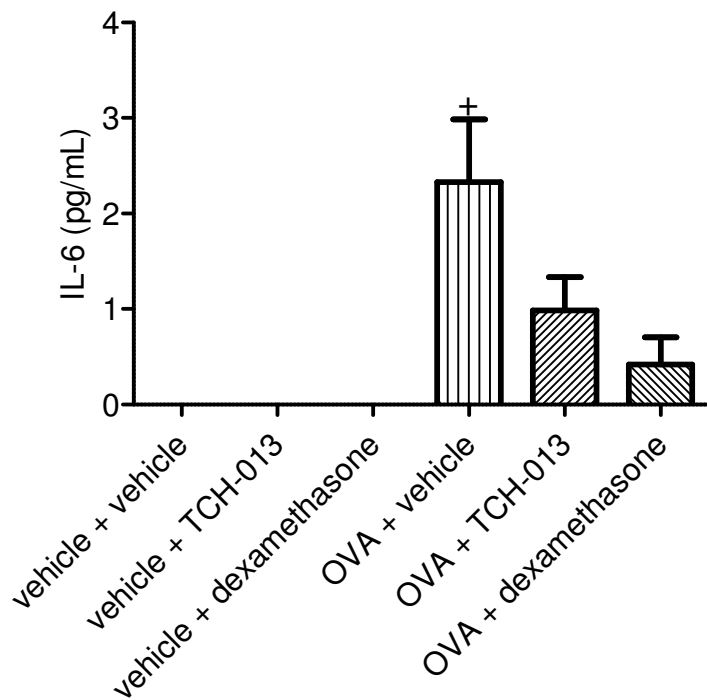


**Figure 12. IL-6 concentration in BALF from OVA or vehicle sensitized mice after treatment with 50 mg/kg TCH-013, vehicle or 0.1 mg/kg dexamethasone.** Treatment with OVA induced a statistically significant increase in IL-6 ( $+p < 0.05$ ,  $n \geq 8$ ). However, treatment with neither TCH-013 nor dexamethasone decreased IL-6 concentration in the BALF ( $p > 0.05$ ,  $n \geq 7$ ).

|                                       | <b>ANOVA with Bonferroni's multiple comparisons test, adjusted P value</b> | <b>ANOVA with Tukey's multiple comparisons test, adjusted P value</b> | <b>T test</b> |
|---------------------------------------|--|---|---------------|
| OVA + vehicle vs. OVA + TCH-013       | 0.1961   | 0.1242  | 0.0927        |
| OVA + vehicle vs. OVA + dexamethasone | 0.0711   | 0.0514  | 0.0745        |
| OVA + TCH-013 vs. OVA + dexamethasone | >0.9999  | 0.9571  | 0.3089        |

**Table 4. Statistical analysis of IL-6 concentration in BALF from select groups of OVA or vehicle sensitized mice after treatment with 50 mg/kg TCH-013, vehicle or 0.1 mg/kg dexamethasone (n ≥ 7).**

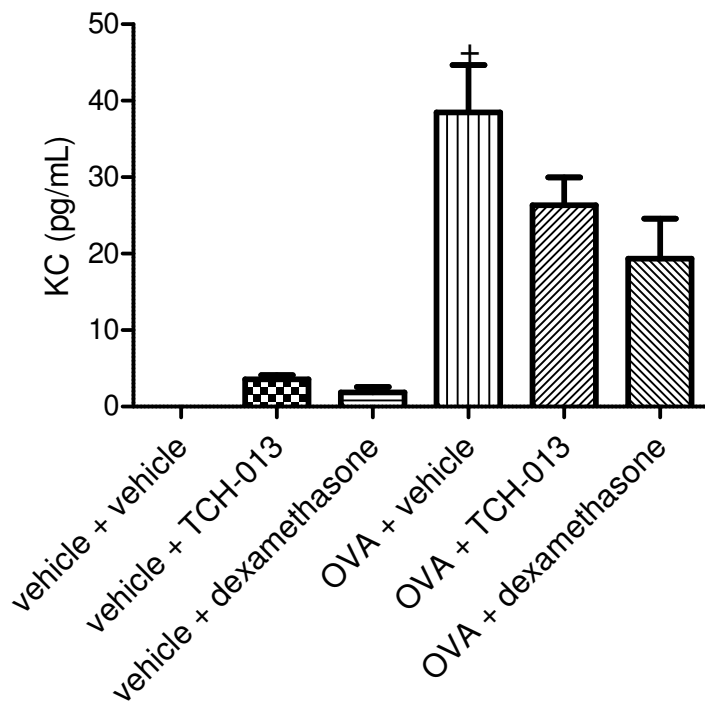


**Figure 13.** KC concentration in BALF from OVA or vehicle sensitized mice after treatment with 50 mg/kg TCH-013, vehicle or 0.1 mg/kg dexamethasone. Treatment with OVA induced a statistically significant increase in KC (+ $p < 0.05$ ,  $n \geq 8$ ). However, treatment with neither TCH-013 nor dexamethasone decreased KC concentration in the BALF ( $p > 0.05$ ,  $n \geq 7$ ).



|                                       | <b>ANOVA with Bonferroni's multiple comparisons test, adjusted P value</b> | <b>ANOVA with Tukey's multiple comparisons test, adjusted P value</b> | <b>T test</b> |
|---------------------------------------|--|---|---------------|
| OVA + vehicle vs. OVA + TCH-013       | 0.3926   | 0.2185  | 0.1160        |
| OVA + vehicle vs. OVA + dexamethasone | 0.0767   | 0.0549  | 0.0719        |
| OVA + TCH-013 vs. OVA + dexamethasone | >0.9999  | 0.9018  | 0.2824        |

**Table 5. Statistical analysis of KC concentration in BALF from select groups of OVA or vehicle sensitized mice after treatment with 50 mg/kg TCH-013, vehicle or 0.1 mg/kg dexamethasone (n ≥ 7).**

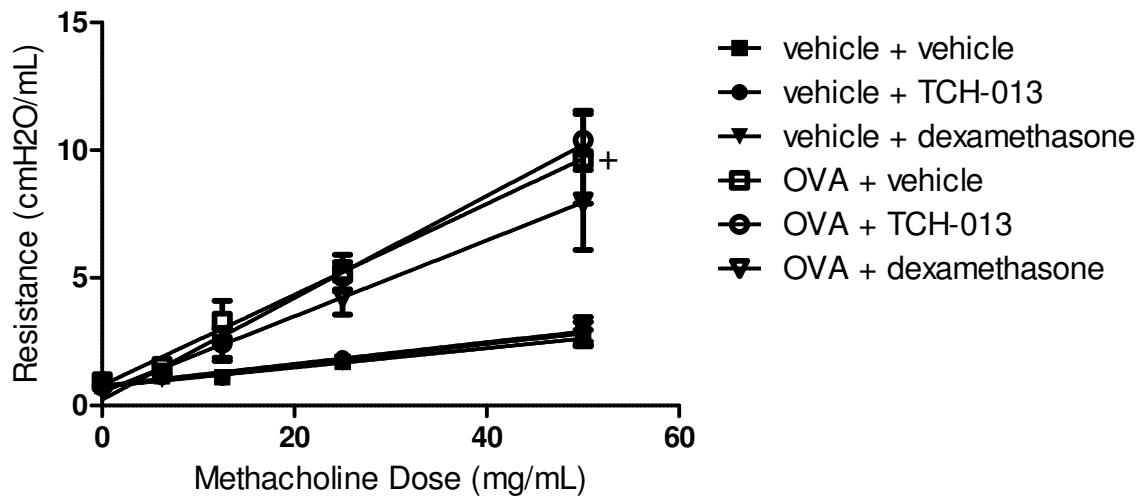


**Figure 14. Total lung resistance after methacholine challenge in OVA or vehicle sensitized mice after treatment with 50 mg/kg TCH-013, saline or 0.1 mg/kg dexamethasone.** OVA sensitization induced airway hyperresponsiveness, measured as resistance using a Flexivent protocol, significantly when compared to vehicle treated mice ( $p < 0.05$ ,  $n \geq 5$ ). Neither TCH-013 nor dexamethasone treatment of the OVA sensitized mice significantly reduced airway hyperresponsiveness when compared to OVA sensitized mice treated with vehicle.

## **Modification of the imidazoline scaffold yielded a molecule with increased efficacy and a noncompetitive binding profile**

In order to optimize the imidazoline scaffold for proteasome inhibition, each of the functional groups on the parent molecule were manipulated and each daughter molecule underwent evaluation *in vitro*. The ability of the compounds to inhibit the chymotryptic-like (CT-L) activity of the 20S proteasome was determined in a purified enzyme system by measuring the rate of hydrolysis of the fluorogenic substrate Suc-LLVY-AMC. Fluorescence increase was measured at 37°C over 30 minutes and the linear portion of the curve was used to measure rates of hydrolysis in response to varying concentrations of drug. Velocity was plotted against log[drug] to generate a dose response curve, from which IC<sub>50</sub> values were determined. Figure 15 shows a curve representative of each curve obtained from the enzyme assay used to calculate IC<sub>50</sub> values.

Building on the parent molecule, TCH-013, domains R<sub>1</sub>-R<sub>3</sub> were the first to be evaluated as potential sites of improvement. A structure-activity analysis led to the determination that, although these groups were necessary for activity, manipulation led to only a modest increase in potency (Table 6). The development of the most potent imidazolines was achieved by synthesizing a compound with the optimal structural features of the compounds from Table 6 and manipulation of the R<sub>4</sub> group (Table 7). Evaluation of these derivatives led to the discovery of compound 46, the first identified noncompetitive proteasome inhibitor with nanomolar potency.<sup>26</sup>

Although the molecule retained the core structural features of TCH-013, the adjustment of the functional groups necessitated evaluation of the kinetic profile of the derivative compounds. In order to determine if these newly identified molecules retained the characteristic noncompetitive binding profile of TCH-013, compound 43 was evaluated. Although slightly less potent than compound 46, the favorable solubility properties as well as the significantly increased potency made compound 43 the ideal candidate for this assessment. Consistent with the reports of TCH-013, the Lineweaver-Burk plot of compound 43 suggests the lines of best fit intersect on the X-axis ( $1/[S]$ ), this pattern is accepted to be representative of a noncompetitive inhibition mechanism (Figure 16).<sup>26,29</sup>

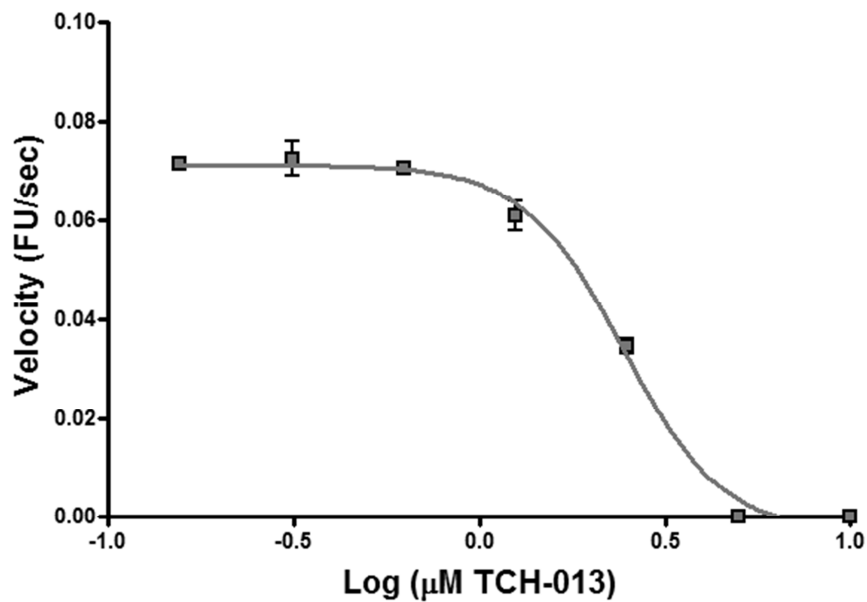
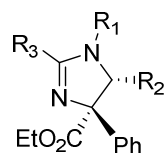


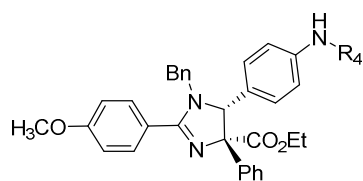
**Figure 15. TCH-013 inhibits the CT-L activity of the human 20S proteasome.** The hydrolysis of the fluorogenic substrate Suc-LLVY-AMC was used to measure the CT-L activity of purified human 20S proteasome. IC<sub>50</sub> values were calculated using GraphPad Prism for Windows, GraphPad Software, San Diego California USA, [www.graphpad.com](http://www.graphpad.com).

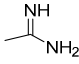
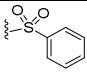
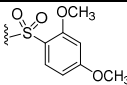
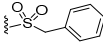
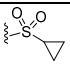
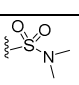
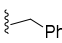
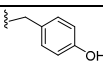
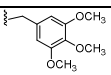
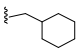


|    | R <sub>1</sub>             | R <sub>2</sub>                            | R <sub>3</sub>             | IC <sub>50</sub> (μM) |
|----|----------------------------|---|----------------------------|-----------------------|
| 11 | H                          | Phenyl                                    | Phenyl                     | >10                   |
| 12 | Acyl                       | Phenyl                                    | Phenyl                     | >10                   |
| 13 | Benzoyl                    | Phenyl                                    | Phenyl                     | >10                   |
| 14 | Tosyl                      | Phenyl                                    | Phenyl                     | >10                   |
| 15 | CH <sub>2</sub> -2-furan   | Phenyl                                    | Phenyl                     | 7.04 <sup>a</sup>     |
| 1  | Benzyl                     | Phenyl                                    | Phenyl                     | 2.58                  |
| 16 | 4-CH <sub>3</sub> O-benzyl | Phenyl                                    | Phenyl                     | 2.73                  |
| 17 | 4-F-benzyl                 | Phenyl                                    | Phenyl                     | 3.71                  |
| 18 | 4-Cl-benzyl                | Phenyl                                    | Phenyl                     | 2.02                  |
| 19 | 4-Br-benzyl                | Phenyl                                    | Phenyl                     | 1.90                  |
| 20 | Benzyl                     | 4-pyridine                                | Phenyl                     | >10                   |
| 21 | Benzyl                     | 2-furan                                   | Phenyl                     | 6.13                  |
| 22 | Benzyl                     | 4-NO <sub>2</sub> -phenyl                 | Phenyl                     | 6.71                  |
| 23 | Benzyl                     | 4-NH <sub>2</sub> - phenyl                | Phenyl                     | 3.52                  |
| 24 | Benzyl                     | 4-CF <sub>3</sub> - phenyl                | Phenyl                     | 4.81                  |
| 25 | Benzyl                     | 4-Cl- phenyl                              | Phenyl                     | 2.23                  |
| 26 | Benzyl                     | 4-NH(SO <sub>2</sub> Ph)-phenyl           | Phenyl                     | 1.08                  |
| 27 | Benzyl                     | 4-SCH <sub>3</sub>                        | Phenyl                     | 2.77                  |
| 28 | Benzyl                     | 4-SO <sub>2</sub> CH <sub>3</sub> -phenyl | Phenyl                     | >10                   |
| 29 | Benzyl                     | 4-NHBenzyl-phenyl                         | Phenyl                     | 0.47                  |
| 30 | Benzyl                     | Phenyl                                    | 4-Br-phenyl                | 3.19                  |
| 31 | Benzyl                     | Phenyl                                    | 4-CH <sub>3</sub> O-phenyl | 1.27                  |
| 32 | Benzyl                     | 4-CN-phenyl                               | 4-CH <sub>3</sub> O-phenyl | >10                   |
| 33 | Benzyl                     | 4-CONH <sub>2</sub> -phenyl               | 4-CH <sub>3</sub> O-phenyl | >10                   |

**Table 6. Inhibition of the chymotryptic-like activity of purified human 20S proteasome by compounds 11-33** ( $n > 2$ , <sup>a</sup> $n = 1$ ). The hydrolysis of the fluorogenic substrate Suc-LLVY-AMC was used to measure the CT-L activity of purified human 20S

**Table 6 (cont'd)** proteasome. IC<sub>50</sub> values were calculated using GraphPad Prism for Windows, GraphPad Software, San Diego California USA, [www.graphpad.com](http://www.graphpad.com).



|    | R <sub>4</sub>  | IC <sub>50</sub> (μM) |
|----|---|-----------------------|
| 34 | H   | 1.97                  |
| 35 | Ac  | 2.17                  |
| 36 | Bz  | 1.44                  |
| 37 |    | 0.63                  |
| 38 |    | 0.58                  |
| 39 |    | 0.53                  |
| 40 |    | 1.08                  |
| 41 |   | 0.91                  |
| 42 |  | 1.22                  |
| 43 |  | 0.30                  |
| 44 |  | 0.54                  |
| 45 |  | 0.37                  |
| 46 |  | 0.13                  |

**Table 7. Inhibition of the chymotryptic-like activity of purified human 20S proteasome by compounds 34-46** (n > 2). The hydrolysis of the fluorogenic substrate Suc-LLVY-AMC was used to measure the CT-L activity of purified human 20S proteasome. IC<sub>50</sub> values were calculated using GraphPad Prism for Windows, GraphPad Software, San Diego California USA, [www.graphpad.com](http://www.graphpad.com).



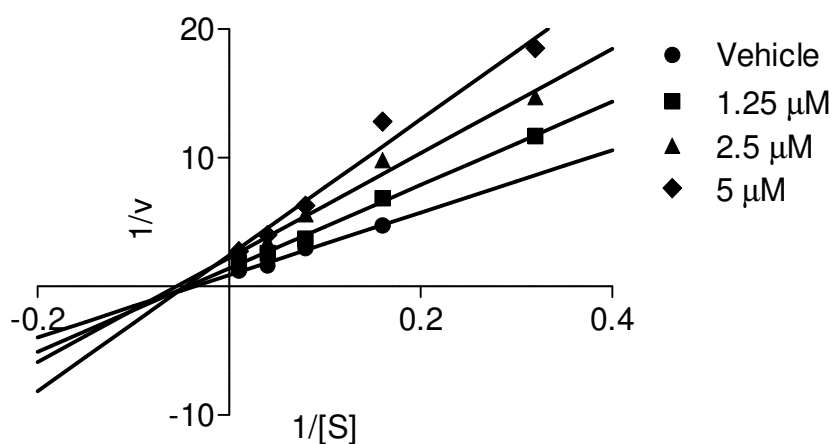


**Figure 16. Kinetic analysis of CT-L activity inhibition by compound 43.** Human 20S proteasome was treated with varying concentrations of the substrate Suc-LLVY-AMC and TCH-013. Hydrolysis of the substrate Suc-LLVY-AMC was used to measure the CT-L activity. A Lineweaver-Burk plot was generated and illustrates a pattern of noncompetitive inhibition. Graphs were generated using GraphPad Prism for Windows, GraphPad Software, San Diego California USA, [www.graphpad.com](http://www.graphpad.com).

## **The modified imidazoline is cytotoxic and overcomes bortezomib resistance in cell culture of multiple myeloma**

Although significant advances have been made in multiple myeloma treatment, the disease remains incurable and almost all patients experience disease relapse.<sup>59</sup> As a method to evaluate the resistant cancer, a model of MM resistance was developed using the human leukemia cell line, THP-1. The mechanism of bortezomib resistance in this model has been attributed to a mutation in the active site of the  $\beta 5$  subunit and the over expression of this mutated protein.<sup>47</sup> Molecules that act via a noncompetitive mechanism may be successful in overcoming bortezomib resistance, because this resistance mechanism is focused on the active site.<sup>25</sup>

The optimized imidazoline compounds were screened for their cytotoxicity against the wild type (WT) and bortezomib resistant (BTZ500) strains of the THP-1 cell line in culture. In the wild type cells, treatment with 10  $\mu$ M imidazoline resulted in cytotoxicity 72 hours after drug administration (Figure 17). In the BTZ500 cells, treatment with 1  $\mu$ M bortezomib treatment exhibited only a modest cytotoxic effect leaving >67% of cells viable. However, the modified imidazoline scaffolds retained their activity at 10 $\mu$ M and overcame resistance, similarly to their parent molecule (Figure 18).<sup>29</sup>

These results indicate that the imidazolines are capable of overcoming bortezomib resistance *in vitro* and act as further evidence that the compounds bind via a distinct mechanism. Further studies elucidating IC<sub>50</sub> values for each of the compounds in cell culture will allow for the calculation of resistance factors and more thorough

evaluation of the cytotoxicity profile. In addition, to assess imidazoline effectiveness in clinical resistance, primary cells obtained from patients with refractory disease should be treated with the imidazolines and evaluated for cytotoxicity.

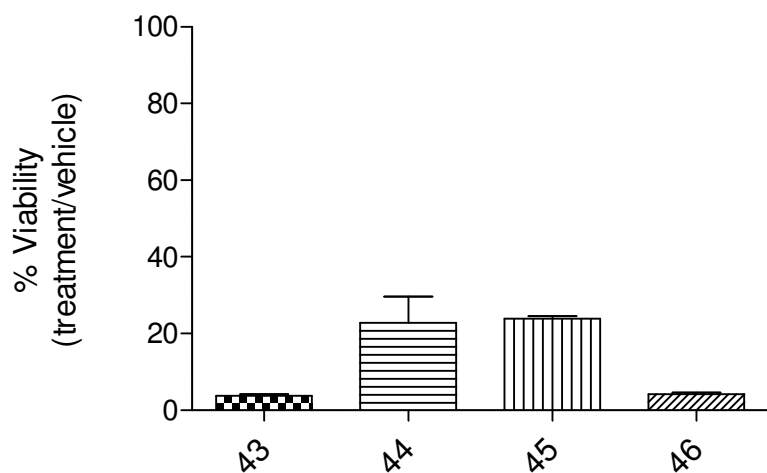


**Figure 17. Cell viability of THP-1 wild type cells after 72 hours of treatment with 10  $\mu$ M imidazoline.** The imidazolines exhibit cytotoxicity against the human leukemia cell line THP-1 after 72 hours of treatment (n = 3).

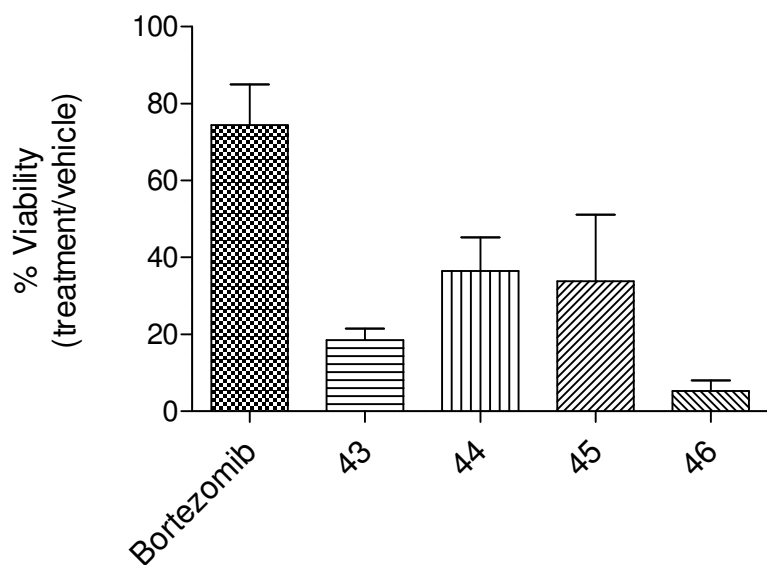


**Figure 18. Cell viability of THP-1 BTZ500 cells after 72 hours of treatment with 10  $\mu$ M imidazoline or 1  $\mu$ M bortezomib.** The imidazoline compounds exhibit cytotoxicity and overcome bortezomib resistance in the human leukemia cell line THP-1 (n = 3).

## **Compound 43 is bioavailable and attenuates the systemic inflammatory response *in vivo***

After determining that compound 43 had a noncompetitive profile and successfully overcame bortezomib resistance, we set out to determine if the lead molecule was bioavailable and could disrupt the systemic inflammatory response.

Intraperitoneal administration of 150 mg/kg of compound 43 in vehicle (30:70 propylene glycol:D5W) resulted in serum concentrations in the high nanomolar range, above the compounds reported IC<sub>50</sub> of 300 nM (Figure 19). These data confirm that the imidazolines, epitomized by compound 43, are bioavailable when administered via IP injection. This preliminary study should be followed up by complex pharmacokinetic studies to determine the comprehensive bioavailability characteristics of compound 43.

Continuing the evaluation of compound 43, the same LPS challenge model of systemic inflammation used to evaluate the parent compound TCH-013 was employed. BALB/c mice with no immunodeficiency were treated with an injection of 50 mg/kg TCH-013 intraperitoneally and one hour later were administered 1 mg/kg LPS. Animals were sacrificed and serum was collected 2 hours after LPS treatment. The results indicate a 50 mg/kg dose of compound 43 significantly reduced serum TNF- $\alpha$  when compared to the vehicle control (Figure 20). LC/MS analysis of serum from these animals revealed compound 43 at  $3.47 \pm 0.41$   $\mu$ M, well above the IC<sub>50</sub> of the compound.

Identification of compound 43 as a nanomolar potency, bioavailable, noncompetitive proteasome inhibitor that can successfully reduce systemic inflammation is the first step toward developing this optimized molecule into a

pharmaceutical candidate. Preliminary data from collaboration with Dr. Terrance Tang at University of Waterloo, ON, CA, showed that oral administration of compound 43 at 100 mg/kg significantly reduces tumor size in a murine xenograft model of multiple myeloma. This is further evidence that these molecules should be approached for their chemotherapeutic potential.

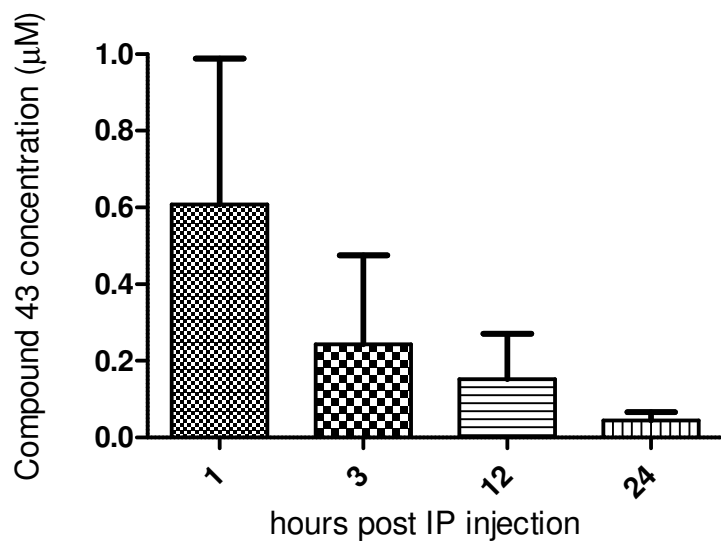


**Figure 19. Compound 43 is present in the serum after IP administration at 150 mg/kg** (n = 4). Animals were given a single IP dose of compound 43 in 30:70 propylene glycol:D5W and blood was drawn at 1, 3, and 12 hours post administration. LC/MS analysis was performed on the samples to determine the quantity of drug present.



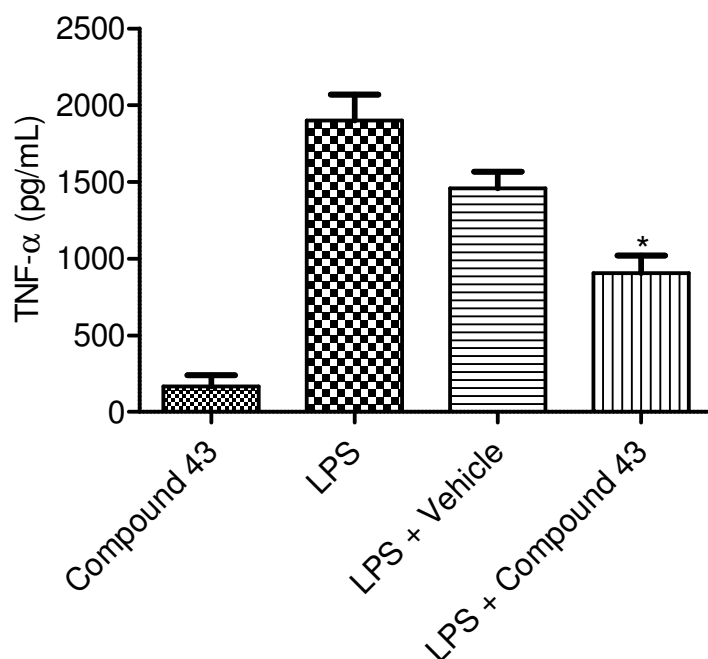


**Figure 20. Compound 43 reduces LPS-induced TNF- $\alpha$  production.** Animals were treated with an IP dose of 50 mg/kg of compound 43, one hour later animals were given an IP dose of 1 mg/kg LPS, and two hours later serum was collected. Concentration of TNF- $\alpha$  in serum was measured using an ELISA. Compound 43 significantly reduces serum TNF- $\alpha$  following LPS challenge when administered at 50 mg/kg IP ( $p < 0.05$ ,  $n > 7$ ).

## CHAPTER 4- SUMMARY AND CONCLUSIONS

### Limitations and Future Directions

There were several limitations in these studies, of particular note are the complex mechanisms involved in the pathogenesis of asthma and the elusiveness of the imidazoline binding site.

It is well documented that the commonly used OVA-induced allergic airway disease is not directly representative of the human specific disease, asthma.<sup>60</sup> Although this model is helpful for studying the pathogenesis of acute airway inflammation, this model has limitations in its predictive value for drug development purposes.<sup>61</sup> In addition, the pathogenesis of asthma is complex and multi-factorial, masking the true effects that the manipulation of NF- $\kappa$ B may have on specific parts of the disease.<sup>62</sup> Further evaluation of the proteasome inhibitor in an experimental model of asthma should be undertaken in conjunction with steroid therapy and with a bronchodilator. Great care should also be taken to determine the effects of the imidazolines on IgE and plasma cells in allergic airway disease. It appears that, even though there may be potential for application of these compounds to asthma; focus should be placed on evaluation of their chemotherapeutic properties.

Although  $\beta 5$  subunit mutation and overexpression has been conclusively linked to bortezomib resistance, the molecular basis for variable clinical response to bortezomib is not well understood.<sup>63</sup> The evaluation of these compounds and the contribution of NF- $\kappa$ B in primary cells from patients with resistant disease would be

helpful to determine if these compounds have potential to overcome multiple bortezomib resistance mechanisms.

In addition, a significant limitation of these studies is the need for further determination of NF- $\kappa$ B inhibition and specificity. Although previous studies have shown that the imidazolines inhibit NF- $\kappa$ B, determination of specific pathway components (I $\kappa$ B, phospho-I $\kappa$ B, and nuclear p65) in both the asthma and bortezomib resistance models is essential.<sup>29</sup>

Compound 43 has shown promising results; however, evaluation of the optimized imidazolines should be expanded. Comprehensive bioavailability and toxicity studies would be the first step toward moving this molecule further along the drug development process. Evaluation of these compounds in the bone marrow microenvironment and in primary cultures from patients with multiple myeloma is essential to complete before this molecule can be considered for clinical potential.

The most significant limitation to these studies is the elusiveness of the imidazoline binding site on the proteasome. Despite evidence indicating that these compounds are noncompetitive inhibitors, determination of the exact binding site is needed to complete the conclusion regarding the mechanism of action of these compounds. Multi-disciplinary experiments are currently underway in the Tepe laboratory in pursuit of binding site identification.

## **Conclusion**

All clinically approved proteasome inhibitors act through a competitive mechanism and result in modulation of NF- $\kappa$ B activity. Although these molecules have

potent anti-cancer and anti-inflammatory properties, they also exhibit dose limiting toxicity and pharmacokinetic issues. The studies presented in this thesis show that the noncompetitive proteasome inhibitor, TCH-013, is bioavailable and not hepatotoxic. This compound was also shown to have anti-inflammatory properties, as evidenced by its ability to reduce TNF- $\alpha$  in the LPS challenge and to reduce the BALF cellularity in an experimental model of asthma. In addition, we showed that efficacy of this molecule could be enhanced by manipulating the functional groups while maintaining its noncompetitive binding profile and anti-neoplastic characteristics. The result of these studies is the discovery of compound 43, a noncompetitive proteasome inhibitor that is able to overcome bortezomib resistance, is bioavailable, and is effective in an animal model of systemic inflammation. These studies illustrate that these imidazoline proteasome inhibitors may be possible alternatives to the classical competitive agents.

Administration of the imidazoline proteasome inhibitors to the complex systems of inflammation and neoplasia clearly modulates the outcomes of these processes, but the precise intracellular mechanism of action needs to be further elucidated. It is my hope that the results and discussion presented in this thesis inspire researchers to further investigate the activity of the imidazolines, with particular emphasis on illuminating how the compounds affect specific intracellular process and inflammatory cascade *in vivo*.

## **BIBLIOGRAPHY**

## BIBLIOGRAPHY

1. Ciechanover A. Intracellular protein degradation from a vague idea through the lysosome and the ubiquitin-proteasome system and on to human diseases and drug targeting: Nobel Lecture, December 8, 2004. *Annals of the New York Academy of Sciences*. Nov 2007;1116:1-28.
2. Voorhees PM, Orlowski RZ. The proteasome and proteasome inhibitors in cancer therapy. *Annual review of pharmacology and toxicology*. 2006;46:189-213.
3. Ostrowska H. The ubiquitin-proteasome system: a novel target for anticancer and anti-inflammatory drug research. *Cellular & molecular biology letters*. 2008;13(3):353-365.
4. Voges D, Zwickl P, Baumeister W. The 26S proteasome: a molecular machine designed for controlled proteolysis. *Annual review of biochemistry*. 1999;68:1015-1068.
5. Gallastegui N, Groll M. The 26S proteasome: assembly and function of a destructive machine. *Trends in biochemical sciences*. Nov 2010;35(11):634-642.
6. Coux O, Tanaka K, Goldberg AL. Structure and functions of the 20S and 26S proteasomes. *Annual review of biochemistry*. 1996;65:801-847.
7. Groll M, Clausen T. Molecular shredders: how proteasomes fulfill their role. *Current opinion in structural biology*. Dec 2003;13(6):665-673.
8. Bedford L, Paine S, Sheppard PW, Mayer RJ, Roelofs J. Assembly, structure, and function of the 26S proteasome. *Trends in cell biology*. Jul 2010;20(7):391-401.
9. Elliott PJ, Zollner TM, Boehncke WH. Proteasome inhibition: a new anti-inflammatory strategy. *Journal of molecular medicine*. Apr 2003;81(4):235-245.
10. O'Connor OA, Moskowitz C, Portlock C, et al. Patients with chemotherapy-refractory mantle cell lymphoma experience high response rates and identical

progression-free survivals compared with patients with relapsed disease following treatment with single agent bortezomib: results of a multicentre Phase 2 clinical trial. *British journal of haematology*. Apr 2009;145(1):34-39.

11. Kisselev AF, van der Linden WA, Overkleeft HS. Proteasome inhibitors: an expanding army attacking a unique target. *Chemistry & biology*. Jan 27 2012;19(1):99-115.
12. Argyriou AA, Iconomou G, Kalofonos HP. Bortezomib-induced peripheral neuropathy in multiple myeloma: a comprehensive review of the literature. *Blood*. Sep 1 2008;112(5):1593-1599.
13. Chen D, Frezza M, Schmitt S, Kanwar J, Dou QP. Bortezomib as the first proteasome inhibitor anticancer drug: current status and future perspectives. *Current cancer drug targets*. Mar 2011;11(3):239-253.
14. Huber EM, Groll M. Inhibitors for the immuno- and constitutive proteasome: current and future trends in drug development. *Angewandte Chemie*. Aug 27 2012;51(35):8708-8720.
15. Dick LR, Fleming PE. Building on bortezomib: second-generation proteasome inhibitors as anti-cancer therapy. *Drug discovery today*. Mar 2010;15(5-6):243-249.
16. Gupta SC, Sundaram C, Reuter S, Aggarwal BB. Inhibiting NF-kappaB activation by small molecules as a therapeutic strategy. *Biochimica et biophysica acta*. Oct-Dec 2010;1799(10-12):775-787.
17. Beck P, Dubiella C, Groll M. Covalent and non-covalent reversible proteasome inhibition. *Biological chemistry*. Oct 2012;393(10):1101-1120.
18. Keats JJ, Fonseca R, Chesi M, et al. Promiscuous mutations activate the noncanonical NF-kappaB pathway in multiple myeloma. *Cancer cell*. Aug 2007;12(2):131-144.
19. Hayden MS, Ghosh S. NF-kappaB, the first quarter-century: remarkable progress and outstanding questions. *Genes & development*. Feb 1 2012;26(3):203-234.

20. O'Neill LA. Targeting signal transduction as a strategy to treat inflammatory diseases. *Nature reviews. Drug discovery*. Jul 2006;5(7):549-563.
21. Rayet B, Gelinas C. Aberrant rel/nfkb genes and activity in human cancer. *Oncogene*. Nov 22 1999;18(49):6938-6947.
22. Nishikori M. Classical and alternative NF- $\kappa$ B activation pathways and their roles in lymphoid malignancies. *Journal of Clinical and Experimental Hematopathology*. 2005;45(1):15-24.
23. Demchenko YN, Kuehl WM. A critical role for the NF $\kappa$ B pathway in multiple myeloma. *Oncotarget*. May 2010;1(1):59-68.
24. Pahl HL. Activators and target genes of Rel/NF-kappaB transcription factors. *Oncogene*. Nov 22 1999;18(49):6853-6866.
25. Li X, Wood TE, Sprangers R, et al. Effect of noncompetitive proteasome inhibition on bortezomib resistance. *Journal of the National Cancer Institute*. Jul 21 2010;102(14):1069-1082.
26. Azevedo LM, Lansdell TA, Ludwig JR, et al. Inhibition of the Human Proteasome by Imidazoline Scaffolds. *Journal of medicinal chemistry*. Jul 3 2013.
27. nobelprize.org. Advanced information on the Nobel Prize in Chemistry. 2004; [http://www.nobelprize.org/nobel\\_prizes/chemistry/laureates/2004/advanced.html](http://www.nobelprize.org/nobel_prizes/chemistry/laureates/2004/advanced.html). Accessed July 3, 2012.
28. Sharma V, Lansdell TA, Peddibhotla S, Tepe JJ. Sensitization of tumor cells toward chemotherapy: enhancing the efficacy of camptothecin with imidazolines. *Chemistry & biology*. Dec 2004;11(12):1689-1699.
29. Lansdell TA, Hurchla MA, Xiang J, et al. Noncompetitive Modulation of the Proteasome by Imidazoline Scaffolds Overcomes Bortezomib Resistance and Delays MM Tumor Growth in Vivo. *ACS chemical biology*. Dec 11 2012.
30. Lansdell TA, O'Reilly S, Woolliscroft T, et al. Attenuation of collagen-induced arthritis by orally available imidazoline-based NF-kappaB inhibitors. *Bioorganic & medicinal chemistry letters*. Jul 15 2012;22(14):4816-4819.



31. Akinbami LJ, Moorman JE, Liu X. Asthma prevalence, health care use, and mortality: United States, 2005-2009. *National health statistics reports*. Jan 12 2011(32):1-14.
32. Hill JM, Tattersfield AE. Corticosteroid sparing agents in asthma. *Thorax*. May 1995;50(5):577-582.
33. Desmet C, Gosset P, Pajak B, et al. Selective blockade of NF-kappa B activity in airway immune cells inhibits the effector phase of experimental asthma. *Journal of immunology*. Nov 1 2004;173(9):5766-5775.
34. Poynter ME, Irvin CG, Janssen-Heininger YM. Rapid activation of nuclear factor-kappaB in airway epithelium in a murine model of allergic airway inflammation. *The American journal of pathology*. Apr 2002;160(4):1325-1334.
35. Levine SJ. NF-kB: A KEY SIGNALING PATHWAY IN ASTHMA. *Signal transduction and human disease*. 2003:23.
36. Yang L, Cohn L, Zhang DH, Homer R, Ray A, Ray P. Essential role of nuclear factor kappaB in the induction of eosinophilia in allergic airway inflammation. *The Journal of experimental medicine*. Nov 2 1998;188(9):1739-1750.
37. Poynter ME, Cloots R, van Woerkom T, et al. NF-kappa B activation in airways modulates allergic inflammation but not hyperresponsiveness. *Journal of immunology*. Dec 1 2004;173(11):7003-7009.
38. Wegmann M, Lunding L, Orinska Z, Wong DM, Manz RA, Fehrenbach H. Long-term bortezomib treatment reduces allergen-specific IgE but fails to ameliorate chronic asthma in mice. *International archives of allergy and immunology*. 2012;158(1):43-53.
39. Elliott PJ, Pien CS, McCormack TA, Chapman ID, Adams J. Proteasome inhibition: A novel mechanism to combat asthma. *The Journal of allergy and clinical immunology*. Aug 1999;104(2 Pt 1):294-300.
40. Alexanian R, Delasalle K, Wang M, Thomas S, Weber D. Curability of multiple myeloma. *Bone marrow research*. 2012;2012:916479.

41. Jemal A, Siegel R, Ward E, Hao Y, Xu J, Thun MJ. Cancer statistics, 2009. *CA: a cancer journal for clinicians*. Jul-Aug 2009;59(4):225-249.
42. Hideshima T, Chauhan D, Richardson P, et al. NF-kappa B as a therapeutic target in multiple myeloma. *The Journal of biological chemistry*. May 10 2002;277(19):16639-16647.
43. Hideshima T, Richardson P, Chauhan D, et al. The proteasome inhibitor PS-341 inhibits growth, induces apoptosis, and overcomes drug resistance in human multiple myeloma cells. *Cancer research*. Apr 1 2001;61(7):3071-3076.
44. Mitsiades N, Mitsiades CS, Poulaki V, et al. Molecular sequelae of proteasome inhibition in human multiple myeloma cells. *Proceedings of the National Academy of Sciences of the United States of America*. Oct 29 2002;99(22):14374-14379.
45. Kumar S, Rajkumar SV. Many facets of bortezomib resistance/susceptibility. *Blood*. Sep 15 2008;112(6):2177-2178.
46. Tsuchiya S, Yamabe M, Yamaguchi Y, Kobayashi Y, Konno T, Tada K. Establishment and characterization of a human acute monocytic leukemia cell line (THP-1). *International journal of cancer. Journal international du cancer*. Aug 1980;26(2):171-176.
47. Oerlemans R, Franke NE, Assaraf YG, et al. Molecular basis of bortezomib resistance: proteasome subunit beta5 (PSMB5) gene mutation and overexpression of PSMB5 protein. *Blood*. Sep 15 2008;112(6):2489-2499.
48. Oeckinghaus A, Hayden MS, Ghosh S. Crosstalk in NF-kappaB signaling pathways. *Nature immunology*. Aug 2011;12(8):695-708.
49. Greenwood KK, Proper SP, Saini Y, et al. Neonatal epithelial hypoxia inducible factor-1alpha expression regulates the response of the lung to experimental asthma. *American journal of physiology. Lung cellular and molecular physiology*. Mar 1 2012;302(5):L455-462.
50. Meng L, Mohan R, Kwok BH, Elofsson M, Sin N, Crews CM. Epoxomicin, a potent and selective proteasome inhibitor, exhibits in vivo antiinflammatory activity. *Proc. Natl. Acad. Sci. U S A*. Aug 31 1999;96(18):10403-10408.

51. Ozer JS, Chetty R, Kenna G, et al. Enhancing the utility of alanine aminotransferase as a reference standard biomarker for drug-induced liver injury. *Regulatory toxicology and pharmacology : RTP*. Apr 2010;56(3):237-246.
52. Wasserman S, Dolovich J, Conway M, Marshall JS. TNF-alpha dysregulation in asthma: relationship to ongoing corticosteroid therapy. *Canadian respiratory journal : journal of the Canadian Thoracic Society*. May-Jun 2000;7(3):229-237.
53. Kumar V, Robbins SL, Cotran RS, MD Consult LLC. Robbins and Cotran pathologic basis of disease. 8th ed. Philadelphia, PA: Saunders/Elsevier,; 2010: <http://ezproxy.msu.edu:2047/login?url=http://www.mdconsult.com/das/book/0/view/2060/1.html>.
54. Gonzalo JA, Lloyd CM, Kremer L, et al. Eosinophil recruitment to the lung in a murine model of allergic inflammation. The role of T cells, chemokines, and adhesion receptors. *The Journal of clinical investigation*. Nov 15 1996;98(10):2332-2345.
55. Barnes PJ. Immunology of asthma and chronic obstructive pulmonary disease. *Nature reviews. Immunology*. Mar 2008;8(3):183-192.
56. Borish LC, Steinke JW. 2. Cytokines and chemokines. *The Journal of allergy and clinical immunology*. Feb 2003;111(2 Suppl):S460-475.
57. Chung KF, Barnes PJ. Cytokines in asthma. *Thorax*. Sep 1999;54(9):825-857.
58. Keller C, Webb A, Davis J. Cytokines in the seronegative spondyloarthropathies and their modification by TNF blockade: a brief report and literature review. *Annals of the rheumatic diseases*. Dec 2003;62(12):1128-1132.
59. Laubach JP, Mitsiades CS, Mahindra A, et al. Management of relapsed and relapsed/refractory multiple myeloma. *Journal of the National Comprehensive Cancer Network : JNCCN*. Oct 2011;9(10):1209-1216.
60. Holmes AM, Solari R, Holgate ST. Animal models of asthma: value, limitations and opportunities for alternative approaches. *Drug discovery today*. Aug 2011;16(15-16):659-670.

61. Stevenson CS, Birrell MA. Moving towards a new generation of animal models for asthma and COPD with improved clinical relevance. *Pharmacology & therapeutics*. May 2011;130(2):93-105.
62. Shen HH, Ochkur SI, McGarry MP, et al. A causative relationship exists between eosinophils and the development of allergic pulmonary pathologies in the mouse. *Journal of immunology*. Mar 15 2003;170(6):3296-3305.
63. Perez-Galan P, Mora-Jensen H, Weniger MA, et al. Bortezomib resistance in mantle cell lymphoma is associated with plasmacytic differentiation. *Blood*. Jan 13 2011;117(2):542-552.